Single cell transcriptional profiling reveals helper, effector, and regulatory MAIT cell populations enriched during homeostasis and activation

Charles Kyriakos Vorkas[1,2†], Chirag Krishna[3†], Kelin Li[4], Jeffrey Aubé[4], Daniel W. Fitzgerald[1,5], Linas Mazutis[6], Christina S. Leslie[3*], Michael S. Glickman[2,7*]

1. Division of Infectious Diseases, Weill Cornell Medicine, Cornell University, NY, NY, USA
2. Immunology Program, Sloan Kettering Institute, Memorial Sloan Kettering Cancer Center, NY, NY, USA
3. Computational and Systems Biology Program, Sloan Kettering Institute, Memorial Sloan Kettering Cancer Center, NY, NY, USA
4. Division of Chemic Biology and Medicinal Chemistry, UNC Eshelman School of Pharmacy, University of North Carolina at Chapel Hill, Chapel Hill, NC, USA
5. Center for Global Health, Weill Cornell Medicine, Cornell University, NY, NY, USA
6. Single Cell Research Initiative, Sloan Kettering Institute, Memorial Sloan Kettering Cancer Center, New York, NY, USA
7. Division of Infectious Diseases, Memorial Sloan Kettering Cancer Center, NY, NY, USA

[†] These authors contributed equally to this manuscript.

* Correspondence: cleslie@cbio.mskcc.org (C.S.L.), glickmam@mskcc.org (M.S.G)

Abstract

Mucosal-associated invariant T (MAIT) cells are innate-like lymphocytes that recognize microbial vitamin B metabolites and have emerging roles in infectious disease, autoimmunity, and cancer. Although MAIT cells are identified by a semi-invariant T cell receptor, their phenotypic and functional heterogeneity is not well understood. Here we present an integrated single cell transcriptomic analysis of over 76,000 human MAIT cells during acute and chronic antigen-specific activation with the MR1 ligand 5-OP-RU and non-specific TCR stimulation. We show that MAIT cells span a broad range of homeostatic, effector, helper, tissue-infiltrating, regulatory, and exhausted phenotypes, with distinct gene expression programs associated with $CD4^+$ or $CD8^+$ co-expression. During acute activation, MAIT cells rapidly adopt a cytotoxic phenotype characterized by high expression of *GZMB*, *IFNG* and *TNF*. In contrast, chronic stimulation induces heterogeneous states defined by proliferation, cytotoxicity, immune modulation, and exhaustion. These scRNAseq-defined MAIT cell subtypes were also detected in individuals recently exposed to *Mycobacterium tuberculosis* infection, confirming their presence during human infection. Our study provides the first comprehensive atlas of human MAIT cells in activation conditions and defines substantial functional heterogeneity, suggesting complex roles in health and disease.

51 **Introduction**

52 Mucosal-associated invariant T (MAIT) cells are a subset of re-circulating innate-like
53 lymphocytes enriched in human liver, lung and gut with highly variable abundance in peripheral
54 blood in healthy donors (<1%-18% in humans)(Godfrey et al., 2019; Li et al., 2018; Vorkas et al.,
55 2018). MAIT cells express an evolutionarily conserved T cell receptor (TCR; TRAV1-2 in humans)
56 that can recognize microbially-derived, non-peptide small molecule metabolites of the vitamin B
57 pathway(Harriff et al., 2018; Treiner et al., 2003) presented by the oligomorphic MHC Ib-related
58 molecule, MR1(Seshadri et al., 2017; Treiner et al., 2003). In contrast to conventional T cells that
59 exit the thymus in a "naive" state and require peptide-specific antigen priming over days to
60 weeks to proliferate, most mature MAIT cells enter the circulation as effector cells and are
61 activated within hours of antigen recognition(Legoux et al., 2019). This innate-like property
62 confers their capacity to be among the first responders to bacterial and fungal pathogens(Dias
63 et al., 2017; Jahreis et al., 2018; Shaler et al., 2017; Vorkas et al., 2018) as well as to viral
64 infections through TCR-independent cytokine stimulation (Lamichhane et al., 2019; Leng et al.,
65 2019; van Wilgenburg et al., 2016).

66

67 Despite a growing body of literature implicating MAIT cells in both homeostasis and
68 disease(Godfrey et al., 2019), their specialized functional states in humans are poorly
69 characterized relative to conventional T cells. For example, whereas conventional T cells are
70 broadly divided into two lineages defined by CD4 or CD8 co-receptor expression and stable
71 functional phenotypes, whether these same lineages can be defined in MAIT cells remains
72 unclear. $CD4^+$ MAIT cells are reported to express increased CD25 and IL2 along with decreased
73 cytotoxic markers relative to $CD8^+$ MAIT
74 cells (Gherardin et al., 2018b; Kurioka et al., 2017; Lamichhane et al., 2019; Vorkas et al., 2018).
75 While $CD8^+$ and $CD4^-CD8^-$ (double-negative; DN) MAIT cells have similar functional

76 phenotypes(Kurioka et al., 2017), the DN subset is reported to have depressed cytotoxic function
77 with increased propensity to activation-induced apoptosis(Dias et al., 2018). Moreover, while
78 prior studies have suggested that MAIT cell functional states may depend on the quality and
79 duration of activating stimuli(Kelly et al., 2019; Lamichhane et al., 2019), the early and late effects
80 of TCR-stimulation on MAIT cell state remain largely unknown.
81
82 Here, we present a single cell transcriptomic atlas of human MAIT cells, comprising more than
83 76,000 cells from peripheral blood under acute and chronic activation with 5-OP-RU or
84 αCD3/CD28 in the presence of IL2 or IL2/TGFβ. Our study elucidates distinct transcriptional
85 programs of $CD4^+$ and $CD8^+$ MAIT cells and identifies novel MAIT cell functional clusters that we
86 validate in human subjects recently exposed to *Mycobacterium tuberculosis*. Our results
87 demonstrate broad functional heterogeneity of MAIT cells and suggest that these innate T cells
88 can participate in complex immune responses in addition to their role in direct killing of
89 pathogens.
90

91

92 **Results**

93 **CD4 or CD8 expression on MAIT cells is associated with distinct transcriptional states**

94 To simulate acute and chronic MAIT cell activation under antigen-specific and non-specific T cell
95 receptor stimulation, we employed an in vitro activation assay using human PBMCs incubated
96 with MR1 ligand (5-OP-RU) or αCD3/CD28 beads for 15 hours (D1; acute) or 7 days (D7; chronic)
97 compared to unstimulated control cells. A subset of conditions at D7 also included TGFβ to
98 further assess potential regulatory phenotypes(Bhattacharyya et al., 2018; Rouxel et al., 2017).
99 Cells were harvested at each time point for flow cytometric assays and flow-cytometry assisted
100 cell sorting (FACS) using MR1 tetramers (Fig. 1a, Supplementary Fig. 1, and Supplementary
101 Table 1). To define the immunologic landscape of MAIT cell states after acute and chronic
102 activation, we performed droplet microfluidics single cell RNA sequencing of these sorted MAIT
103 cells from the peripheral blood of three donors in the activation conditions defined above. 76,845
104 MAIT cells passed quality control and were used for downstream analysis.

105

106 Although prior studies have demonstrated that MAIT cells can express CD4 or CD8 co-
107 receptors(Gherardin et al., 2018b; Kurioka et al., 2017; Vorkas et al., 2018), it is unclear whether
108 these markers define functionally distinct MAIT cell populations. We first sought to resolve this
109 question using our single cell data by performing a differential expression analysis between
110 $CD4^+CD8^-$ and $CD4^-CD8^+$ MAIT cells at D1 (Fig. 1b,c) or D7 (Fig. 1d, e) in the absence of TCR
111 stimulation. At D1 (Fig. 1c) $CD4^+$ MAIT cells more highly express genes associated with
112 conventional naïve and central memory T cells including *LEF1*, *SELL*, and *CCR7*, but also
113 markers of activation and co-stimulation such as *CTLA4*, *IL2RA*, *TNFRSF4*, and *TNFRSF18* (Fig
114 1b, Supplementary Table 2). $CD8^+$ MAIT cells more highly express markers of cytotoxic activity
115 such as *NKG7*, *KLRD1*, *EOMES*, *GNLY*, and *GZMB* as well as the transcription factor *RORA*.

116 We confirmed the differential expression of CD25, OX40, GZMB, and EOMES at the protein level
117 within $CD4^+$, $CD8^+$, DN and $CD4^+CD8^+$ (double-positive; DP) MAIT cell subsets using flow
118 cytometry (Fig. 1c). At D7, $CD4^+$ MAIT cells upregulated *CTLA4*, *TNFRSF4*, *SELL*, *IL2RA* and
119 *CCR7*, whereas $CD8^+$ MAIT cells upregulated *NKG7*, *GZMA*, *GZMK*, *PRF1*, SLAMF7 as well as
120 several genes involved in Type I interferon signaling (*IFI44L*, *IFITM3*, *IFI6*, *IFITM1*, and *ISG15*)
121 (Fig. 1d, Supplementary Table 3). We confirmed the differential expression of OX40, CTLA4,
122 GZMA, and GZMK in each subset at the protein level (Fig. 1e). Our analysis demonstrates that
123 $CD4^+$ MAIT cells are associated with expression of co-stimulatory receptors, IL2 signaling and
124 memory markers, whereas $CD8^+$ MAIT cells are defined by granzyme-mediated cytotoxicity and
125 type 1 interferon signaling. These results suggest that CD4 and CD8 expression on MAIT cells
126 may define distinct functional roles.
127
128 **Single cell transcriptional analysis defines heterogeneous MAIT cell activation states**
129 To fully characterize the phenotypic states of tetramer positive MAIT cells, we performed
130 dimensionality reduction by principal component analysis followed by Louvain clustering on cells
131 from all donors, timepoints, and stimuli (Fig. 2a). Clusters were broadly partitioned by timepoint
132 (Supplementary Fig. 2). Visualization with uniform manifold approximation and projection
133 (UMAP) together with differential expression analysis displayed 12 clusters that could be
134 distinguished by homeostatic, cytotoxic, Th1-associated cytokine release, proliferating, tissue-
135 infiltrating, immune regulatory, and exhausted states (Fig. 2b-c; Supplementary Table 3).
136 Clusters 1-3 were enriched at D1 (acute activation). Cluster 1 (C1) had high expression of *IFNG*,
137 *GZMB*, *TNF*, *TBX21*, and notably the transcription factor *FOXP3*. Since this cluster expressed
138 genes associated with granzymes and Th1-associated cytokines, it was termed "MAIT1
139 cytotoxic effector" (Koay et al., 2019), consistent with a similar cluster detected in Koay *et*
140 *al*.(Koay et al., 2019) C2 demonstrated increased *CD69* and pronounced expression of heat

141 shock proteins, *NR4A1*, and the AP-1 subunits *JUN* and *FOS* and was named “Early activated”.
142 C3 expressed effector/central memory markers *CCR7* and *C62L*, markers of MAIT cell
143 intrathymic development *CD4* and *LEF1*(Koay et al., 2019), as well as *RUNX3*. This cluster also
144 upregulated type 1 interferon signaling genes, e.g. *IFIT3* and *ISG15*. Thus, C3 was named “ISG$^+$
145 memory” (ISG: interferon-stimulated genes). Collectively these clusters define the landscape of
146 MAIT cells during homeostasis and early activation. The rapid induction of cytotoxic effector
147 programs at this timepoint suggest that MAIT cells may be poised to respond earlier than
148 conventional T cells.
149
150 In contrast, clusters 4-12 were enriched with chronic activation and demonstrated marked
151 phenotypic heterogeneity. C4 and C5 (“Homeostatic effectors”) displayed similar expression
152 patterns, with high levels of *IL7R*, *GZMM*, *GZMK*, *KLRG1* and *IFI44L* and decreased expression
153 of *CD69* and *CD25*. C4 was distinguished from C5 by expression of vascular endothelial growth
154 factors *VEGFA/B* and was named "Homeostatic effector VEGF." C6 ("Degranulating effector”)
155 showed high expression of *LAMP1*, cytokines *TNF* and *TNFSF13B* (B-cell activating factor),
156 *IFNGR1*, as well as the homing molecule *CXCR3*. C7 ("MR1$^+$ MAIT17") expressed *GZMA*,
157 *ENTPD1*, *RORA*(Koay et al., 2019) as well as *MR1* itself, suggesting that this population may
158 interact with other MAIT cells. C8 ("Tissue-infiltrating-like") highly expressed *ITGA1* and *ITGAE*
159 and was only present in activation conditions including TGFβ. C9 was termed “Innate-like” given
160 its high expression of *HOPX*, *KLRB1*, and *NCR3* together with *GZMA* and *GZMK*. Clusters 10-
161 12 were defined by a gradient of activation/exhaustion marker expression including *PDCD1*,
162 *CTLA4*, *PDCD1* and *LAG3*, with C12 ("Late activated/exhausted") resembling a terminally
163 exhausted population. C11 ("Proliferating") demonstrated a strong mitotic phenotype. C10
164 ("Cytotoxic/Regulatory") upregulated *GZMA*, *GNLY* and *IL26* as well as immune modulating
165 genes *TGFβ* and *LAG3*. Taken together, these analyses define a highly diverse MAIT cell

166 transcriptional landscape shaped by chronic activation, with important parallels with
167 conventional $CD4^+$ and $CD8^+$ T cells.
168
169 **Acute MAIT cell activation induces a cytotoxic phenotype marked by GZMB, IFNG, and**
170 **TNF**
171 We next asked how the prevalence of these populations varied across stimuli and donors during
172 acute and chronic activation (Fig. 2d-e and Supplementary Fig. 2b). In particular, C1 "MAIT1
173 cytotoxic effector"—which expressed high levels of *IFNG*, *GZMB*, and *TNF*—was enriched by
174 TCR stimulation conditions with 5-OP-RU or αCD3/CD28 compared to cells incubated with IL2
175 alone (Fig. 3a, b). To validate and further explore these early transcriptional phenotypes, we
176 performed flow cytometric characterization of MAIT cells under the same acute activation
177 conditions.
178
179 First, we confirmed the differential expression of common T cell surface activation markers IL7R,
180 CD69, and CD25 (Fig. 3c). Unexpectedly, IL7R was significantly downregulated by 5-OP-RU, but
181 not αCD3/CD28. CD69 and CD25 were significantly upregulated by both stimulation conditions,
182 though CD69 was more highly expressed with aCD3/CD28, likely indicating the relative potency
183 of this non-specific T cell stimulus. These results demonstrate that MAIT cells rapidly adopt
184 distinct immune phenotypes after acute antigen-specific and non-specific TCR stimulation.
185
186 As *GZMB*, *IFNG*, and *TNF* were significantly upregulated in early activation clusters C1 and C2,
187 we next asked if these markers were co-expressed at the protein level. A representative gating
188 strategy of intracellular co-staining for GZMB, IFNγ and TNF is presented alongside cumulative
189 data from 30 healthy donors (Fig. 3d). These analyses confirmed the presence of a MAIT cell
190 population with a combined granzyme and Th1-associated cytokine phenotype enriched with

191 acute activation, consistent with "MAIT1 cytotoxic" C1 enriched in the αCD3/CD28 condition in
192 the single cell RNA-seq analysis. The primary acute activation response in MAIT cells was
193 upregulation of granzyme B alone, which was increased in αCD3/CD28 relative to 5-OP-RU
194 conditions (Fig. 3d). 5-OP-RU and αCD3/CD28 both induced significant co-expression of GZMB
195 and TNFα, though increased co-expression was observed with αCD3/CD28 (Fig. 3d). Only
196 αCD3/CD28 induced IFNγ and TNFα co-expression (Fig. 3d). These results are consistent with
197 increased expression of IFNγ and TNFα with non-specific TCR stimulation.
198
199 We next performed a differential expression analysis between MAIT cells stimulated with 5-OP-
200 RU and aCD3/CD28 at D1 to define the gene expression programs associated with antigen-
201 specific or non-specific TCR stimulation (Fig. 3e and Supplementary Table 4). Although both
202 acute TCR-stimulation conditions induced similar transcriptional states (Fig. 2d), we did detect
203 stimulus-specific gene expression patterns, with αCD3/CD28 robustly upregulating *GZMB*,
204 *PRF1*, *IFNG*, *IL2RA*, *BATF3*, *CTLA4*, and *LAG3*. In contrast, 5-OP-RU induced a strong type 1
205 interferon signaling signature with upregulation of *IFIT1*, *ISG15*, *IFI44L*, *IFIT3*, *IFITM1* and *IFI6*.
206 These findings are consistent with distinct MAIT cell transcriptional programs driven by acute
207 antigen-specific signals versus non-specific T cell stimulation.
208
209 **MAIT cells upregulate FOXP3 during acute and chronic activation**
210 Given differential expression of *FOXP3* observed in C2, we sought to further characterize
211 peripheral FOXP3 expressing MAIT cell subsets by flow cytometry. Although few FOXP3^{+} MAIT
212 cells were detected in resting cells, FOXP3 protein was significantly upregulated with 5-OP-RU
213 and αCD3/CD28 during acute stimulation (Fig. 4a,b). In contrast, only 5-OP-RU significantly
214 upregulated FOXP3 during chronic stimulation (Fig. 4b).

215

216 As FOXP3 is a transcriptional regulator of $CD4^+$ regulatory T (Treg) cells and often co-expressed
217 with CD25(Liston et al., 2008; Yamaguchi et al., 2011), we hypothesized that MAIT cells could
218 share similar staining characteristics. First, we compared FOXP3 expression in $CD4^+$ and $CD8^+$
219 MAIT cells with non-MAIT $CD4^+$ T cells (Fig. 4c). While $CD4^+$ MAIT cells had increased FOXP3
220 expression at baseline, only chronic 5-OP-RU-activated $CD8^+$ MAIT cells stably upregulated
221 FOXP3 (Fig. 4c). The addition of TGFβ did not significantly affect MAIT cell FOXP3 expression,
222 though there was a trend for increased $FOXP3^+$ expression with TGFβ co-stimulation (Fig. 4c).
223 We next compared FOXP3/CD25 co-expression in MAIT cells with non-MAIT $CD4^+$ T cells and
224 found that 5-OP-RU-activated MAIT cells strongly upregulated FOXP3, but CD3/CD28
225 stimulation only upregulated FOXP3 in conventional $CD4^+$ T cells (Fig. 4d). In contrast to Treg
226 cells, the $FOXP3^+CD25^+$ MAIT cells were strongly induced in the $CD8^+$ MAIT cell subset after 5-
227 OP-RU activation (Fig. 4e). As previously reported(Hoffmann et al., 2004), αCD3/CD28
228 stimulation alone resulted in significant Treg cell expansion (Fig. 4e). Analysis of absolute
229 numbers of $FOXP3^+CD25^+$ MAIT cells demonstrate that $FOXP3^+CD25^+$ MAIT cells were most
230 prevalent within the $CD8^+$ MAIT cell subset (Fig. 4f) and that the vast majority of FOXP3
231 expressing cells were detected among $CD25^+IL7R^-$ cells and rarely among $CD25^-$ cells (Fig. 4g).
232

233 **Chronic activation of MAIT cells expands homeostatic subpopulations while also inducing**
234 **proliferative, cytotoxic, regulatory, and exhausted phenotypes**

235

236 We next examined clusters enriched during chronic activation (Fig. 5a). These clusters were
237 broadly associated with expression of *MKI67*, *GZMA*, *GZMB*, *TNF*, *CTLA4*, *ICOS*, *LAG3*, *FAS*,
238 and *PDCD1* (Fig. 5a-b). Despite largely overlapping transcriptional states observed between
239 chronic 5-OP-RU and αCD3/CD28 conditions (Fig. 2e), 5-OP-RU significantly upregulated genes

240 associated with lymphoid development (*LTB*), self-renewal (*LST1*), maturation (*CD52*), motility
241 and proliferation (*STMN1*, *ACTG1*) and recruitment of immune cells (*CCL3*, *CCL4*)
242 (Supplementary Table 4). In contrast, αCD3/CD28 upregulated genes associated with
243 cytotoxicity (*GZMB*, *GZMK*), cell stress (*HILPDA*), and exhaustion (*CTLA4*, *LAG3*)
244 (Supplementary Table 4). This granzyme/exhaustion signature observed was largely driven by
245 C12 defined by cells from Donor 1 (Supplementary Fig. 2c).
246
247 The transcriptional differences between stimuli were further elucidated at the protein level, where
248 proliferation marker Ki67 was significantly upregulated in the 5-OP-RU but not the αCD3/CD28
249 condition (Fig. 5c,d). This was consistent with robust antigen-specific MAIT cell expansion not
250 observed with chronic αCD3/CD28 (Fig. 5e). Similar to acute activation, we again detected
251 significant downregulation of IL7R at the protein level only in the 5-OP-RU condition, which was
252 associated with significant upregulation of CD25 not observed with chronic αCD3/CD28
253 stimulation (Fig. 5f). Similar to acute activation, GZMB was the dominant MAIT cell effector
254 protein (Fig. 5g). Activation/exhaustion markers CTLA4, PD1, FAS, ICOS and LAG3 expression
255 were also enhanced with chronic 5-OP-RU stimulation at the protein level (Fig. 5g).
256
257 **MAIT cell subtypes are present during human tuberculosis infection**
258
259 Finally, we assessed whether the MAIT cell phenotypes observed during acute and chronic
260 activation could also be detected during natural human exposure to *Mycobacterium tuberculosis*
261 (*Mtb*). To this end, we analyzed MAIT cell phenotypes in PBMCs collected from household
262 contacts of active TB patients in Port-au-Prince, Haiti compared to healthy unexposed donors
263 from the same community.
264

265 First, we focused our analysis on a subset of markers that characterized $CD4^+$ MAIT cells in our
266 single cell analyses. We observed a similar differential expression pattern of CD25, CCR7 and
267 OX40 at the protein level in $CD4^+$ MAIT cells relative to other subsets (Fig. 6a-c). Moreover, each
268 of these markers was significantly upregulated in contacts recently exposed to *Mtb,* indicating
269 that the acute activation gene expression pattern characteristic of clusters 1-3 in vitro
270 correspond to in vivo MAIT cell subsets in the context of recent *Mtb* exposure. Consistent with
271 our previous work(Vorkas et al., 2018), these findings indicate that $CD4^+$ MAIT cells respond to
272 acute *Mtb* exposure.
273
274 We next interrogated MAIT cell FOXP3 expression, which was predominant in the $CD8^+$ subset
275 after chronic antigenic stimulation (Fig. 4e,f). We found that recently exposed contacts
276 expressed increased FOXP3 relative to healthy controls (Fig. 6d). Consistent with the scRNA-
277 seq results, $FOXP3^+CD25^+$ MAIT cells were most prevalent in the $CD8^+$ subset, and
278 $FOXP3^+CD25^+$ $CD8^+$ MAIT cells were significantly enriched in contacts (Fig. 6e). When stratifying
279 by *Mtb*-specific IFNγ release assay (IGRA) status, which distinguishes contacts who were
280 exposed and latently infected (IGRA+) from those who remained uninfected (IGRA-), we
281 observed that $FOXP3^+CD25^+$ $CD8^+$ MAIT cells were enriched in latently infected contacts (Fig.
282 6f), further confirming that this MAIT cell subtype is responding to *Mtb* infection. These MAIT
283 cell phenotypes detected in TB contacts closely resemble the $CD8^+FOXP3^+CD25^+$ MAIT cells
284 detected with antigen specific stimulation residing in clusters 1-3 (Fig. 3 and 4) and indicate that
285 these cell states defined by single cell transcriptomics are present during acute human *Mtb*
286 exposure and infection.
287
288 **Discussion**

289 MAIT cells have been well-characterized as innate-like, rapid responders to microbial antigens
290 with the capacity to mount cytotoxic responses and secrete Th1/Th17-associated cytokines
291 within hours of antigen recognition(Dias et al., 2017; Dusseaux et al., 2011; Vorkas et al., 2018).
292 However, less is known about the transcriptional programs that define MAIT cell adaptation
293 during acute and chronic activation states. Here we provide the first single cell transcriptional
294 atlas of over 76,000 human MAIT cells in homeostatic and acute/chronic activation states
295 coupled with flow cytometric and functional characterization. Our analysis demonstrates distinct
296 transcriptional programs defined by incubation period and quality of stimulus, revealing novel
297 MAIT cell subpopulations not yet described by bulk RNA-seq or traditional flow cytometric
298 approaches.
299
300 First, our work contributes further evidence to support divergent transcriptional and functional
301 phenotypes associated with human MAIT cell CD4 or CD8 co-expression. Several prior studies
302 have used CD8 as a prerequisite for defining MAIT cells or did not distinguish between
303 subsets(Coulter et al., 2017; Estevez et al., 2020; Koay et al., 2019; Slichter et al., 2016).
304 Differential expression analysis revealed that $CD4^+$ MAIT cells upregulated *IL7R*, *CD25*, *CCR7*,
305 *SELL* along with TNF superfamily receptors *TNFRSF4* and *TNFRSF18*, suggesting that $CD4^+$
306 MAIT cells respond to distinct co-stimulatory signals from the $CD8^+$ subset. We hypothesize
307 that this $CD4^+$ MAIT cell signature may confer unique tissue-homing functions through *CCR7*
308 and *SELL*. Future studies will help to evaluate whether this $CD4^+$ MAIT cell signature confers the
309 capacity to exit the circulation and migrate into tissues.
310
311 Recent work in mice and humans shows that CD4 and the transcription factor, LEF1, are co-
312 expressed during MAIT cell intrathymic development with reciprocal downregulation of CD319
313 (SLAMF7)(Koay et al., 2019). CD4 is subsequently downregulated as MAIT cells mature with

314 reciprocal upregulation of CD8 and CD319 during thymic egress. In a parallel observation in
315 human peripheral blood MAIT cells, we observed that $CD4^+$ MAIT cells significantly upregulated
316 *LEF1*, while *SLAMF7* was significantly differentially expressed in $CD8^+$ MAIT cells. We
317 hypothesize that the peripheral $CD4^+$ MAIT cells may comprise newly generated cells emigrating
318 from the thymus(Fink and Hendricks, 2011). Our findings motivate further study of how MAIT
319 cell activation conditions can select for CD4 or CD8 co-expression in peripheral circulating
320 populations, and further, how these subsets differentially respond to major pathogens. Indeed,
321 our TB data demonstrate that CD25, CCR7 and OX40 are significantly upregulated in $CD4^+$ MAIT
322 cells of TB contacts, suggesting that this subset responds to acute *Mtb* exposure.
323
324 The second aim of our study was to distinguish between transcriptional phenotypes induced
325 during acute and chronic activation and to characterize functional programs associated with
326 MR1 ligand vs non-specific T cell stimulation. We observed that acutely activated MAIT cells
327 with either stimulus were driven towards similar states defined by a rapid upregulation of GZMB,
328 IFNγ and TNFα. At both the transcript and protein level, this signature was more potently
329 induced by αCD3/CD28, which is possibly explained by non-specific stimulation of all T cells
330 within PBMCs triggering cytokine release by MAIT and non-MAIT T cells alike(Trickett and Kwan,
331 2003). αCD3/CD28 may mimic other non-specific T cell stimuli derived from whole bacteria or
332 cytokines, which have previously been shown to significantly upregulate GZMB and IFNγ in MAIT
333 cells relative to 5-OP-RU alone(Lamichhane et al., 2019; Suliman et al., 2019). In contrast, acute
334 activation with 5-OP-RU induced a strong type I interferon-driven gene expression phenotype
335 along with T cell maturation marker CD52. Co-stimulation of MAIT cells with 5-OP-RU and type
336 1 interferons have previously been shown to enhance GZMB and IFNγ release(Lamichhane et
337 al., 2020). Our results demonstrate that acute antigen stimulation alone also enhances MAIT cell
338 type 1 interferon immunity, which may promote survival and proliferation observed during

339 chronic stimulation(Welsh et al., 2012) as well as modulate immunity against bacterial or viral
340 pathogens.(Trinchieri, 2010)
341
342 While previous studies have used chronic 5-OP-RU co-stimulation to expand MAIT cells for
343 downstream use during in vitro functional assays(Boulouis et al., 2020; Gherardin et al., 2018a),
344 this is the first investigation of the transcriptional landscape of chronic antigen-specific activation
345 during this proliferative phase. While we observed largely overlapping transcriptional signatures
346 between 5-OP-RU and αCD3/CD28 activation conditions, 5-OP-RU significantly upregulated
347 genes associated with T cell development, self-renewal, proliferation and recruitment of
348 inflammatory cells. In contrast, chronic αCD3/CD28 activation upregulated genes associated
349 with cytotoxicity, stress and exhaustion. These differences between antigen and mitogen
350 stimulation were recapitulated by flow cytometry. Taken together, these results demonstrate
351 that antigen-specific stimulation is required for MAIT cell survival, expansion and sustained
352 effector function during the chronic phase of stimulation.
353
354 Moreover, we describe a $FOXP3^+$ peripheral blood MAIT cell subset enriched in acute activation
355 cluster C1 with abundant FOXP3 detected at the protein level during chronic 5-OP-RU
356 stimulation. We observed that peripheral $FOXP3^+$ induction was detected almost exclusively in
357 the $CD8^+CD25^+IL7R^-$ subset, in contrast to a recent study(Ling et al., 2016). This surface co-
358 expression of FOXP3 and CD25 in $CD8^+$ MAIT cells parallels that of $CD4^+$ Treg cells and raises
359 the question of whether FOXP3 expression in MAIT cells may confer a similar immune regulatory
360 function(Bhattacharyya et al., 2018). Importantly, we extend our findings of MAIT cell FOXP3
361 induction in vitro to immune responses of donors recently exposed to *Mtb*. We found that $CD8^+$
362 $FOXP3^+CD25^+$ MAIT cells accumulated after acute *Mtb* exposure in healthy household TB

363 contacts and were significantly more abundant in recently infected donors (IGRA+ contacts).
364 Our results suggest that $CD8^+$ $FOXP3^+CD25^+$ MAIT cells respond to acute *Mtb* infection.
365
366 In addition to FOXP3 expression, our analysis identifies several alternative immune regulatory
367 mechanisms mediated by MAIT cells. We observed that activation/exhaustion marker LAG3 was
368 significantly upregulated in chronically activated MAIT cell clusters (C7, C10, and C12) and was
369 significantly differentially expressed in $CD8^+$ and DP subsets. LAG3 can bind peptide-MHC II
370 complexes and inhibit $CD4^+$ T cell activation(Maruhashi et al., 2018). Additionally, MAIT cells
371 may target $CD4^+$ T cells via MR1 or through secretion of immunomodulatory cytokines like TGFβ.
372 Future studies will help to elucidate the relative contribution of these immune modulation
373 pathways on MAIT cell regulatory activity.
374
375 Our study also highlights that MAIT cell activation rapidly drives phenotypic and functional
376 exhaustion. This was evident in both antigen and non-specific stimulation conditions at the
377 transcriptional and protein level. These findings mirror evidence from chronic disease states
378 such as TB, viral hepatitis, and malignancy where increased MAIT cell PD1 expression is
379 associated with peripheral MAIT cell depletion and dysfunction and directly correlates with
380 severity of disease in some studies (Duan et al., 2019; Hengst et al., 2016; Jiang et al., 2020;
381 Leeansyah et al., 2013; Saeidi et al., 2015; Shaler et al., 2017; Yong et al., 2018). While immune
382 checkpoint molecules can be transiently upregulated after T cell activation, we observed
383 sustained expression in chronic activation clusters. At the protein level, these exhaustion
384 markers were significantly upregulated in the 5-OP-RU condition, suggesting that chronic
385 antigen-specific activation strongly induces negative feedback mechanisms to suppress further
386 activation and proliferation. Taken together, these data imply that checkpoint blockade may
387 enhance MAIT cell activity against infectious or malignant disease (Boulouis et al., 2020;

388 Leeansyah et al., 2015; Venken et al., 2018) or contribute to autoimmune complications of
389 immunotherapy(Sasson et al., 2020).
390
391 We acknowledge certain limitations to our study. The foremost of these is the small number of
392 individuals in our single cell cohort and donor-to-donor variability. However, the functional flow
393 cytometric validation in multiple donors, including a genetically distinct population from Haiti,
394 strengthens our confidence that the MAIT cell states observed can be applied to other
395 populations. Future studies will test the reproducibility of this transcriptional atlas in additional
396 healthy donors or in specific disease states.
397
398 In sum, we present an integrated transcriptional and immune landscape of human MAIT cell
399 activation at single cell resolution. Our results provide a detailed analysis of novel MAIT cell
400 clusters defined by acute and chronic stimulation, including distinct $CD4^+$ and $CD8^+$ MAIT cell
401 signatures. We also show that these phenotypes are recapitulated in the setting of acute *Mtb*
402 exposure and infection. This functional map of MAIT cell activation biology will help inform future
403 investigations into how MAIT cells specialize in healthy and disease states.
404
405 **Acknowledgments**
406
407 We would like to thank Ojasvi Chaudhury for his assistance in single-cell RNA-seq libraries
408 preparation. We acknowledge the Immune Monitoring, Flow Cytometry, and Integrated
409 Genomics Operation Core Facilities at the Sloan Kettering Institute, Memorial Sloan Kettering
410 Cancer, NY, NY for their expert consultation and services rendered during this project. We also
411 acknowledge the NIH Tetramer Core (Emory University, Atlanta, GA) for providing MR1
412 tetramers. This work was supported by the Ludwig Center for Cancer Immunotherapy, the Tri-I

413 TBRU, part of the TBRU Network (U19 AI111143), and P30 CA008748. L.M. acknowledges
414 support by The Alan and Sandra Gerry Metastasis and Tumor Ecosystems Center. C.K.V. was
415 supported by NIH NIAID K08 AI132739.
416

417 **Conflicts of interest:**

418 M.S.G. reports consulting fees and equity in Vedanta Biosciences, Inc., consulting fees from
419 Takeda, and is on the SAB of PRL-NYC.
420

421 **Author Contributions**

422 C.K.V. and M.S.G. conceived of the study. C.K.V. conducted the experiments. J.A. and K.L.
423 synthesized 5-A-RU. L.M. conducted inDROP scRNA-seq. D.F.W. recruited the Haitian TB
424 contact cohort. C.K. and C.S.L. analyzed single-cell RNA sequencing data. C.K.V., C.K., C.S.L.
425 and M.S.G. analyzed wrote the manuscript with input from all authors.
426
427

428 **Methods**

429 **PBMC collection**

430 Healthy donor PBMCs were obtained with written informed consent at Sloan Kettering Institute,
431 MSKCC, Rockefeller University or ATCC. De-identified blood samples were processed
432 according to the protocols approved by the Institutional Review Board of MSKCC and
433 Rockefeller University. TB household contacts and unexposed community controls were
434 recruited at GHESKIO centers, Port-au-Prince, Haiti (U01AI069421). PBMCs were isolated from
435 peripheral blood using Ficoll-Prep (GE Healthcare) or cell preservation tubes (CPT; Becton
436 Dickinson) according to the manufacturer's instructions and cryopreserved using 90% fetal

437 bovine serum (Gibco) 10% DMSO (Sigma Aldrich) and stored in liquid N_2 prior to thawing for in
438 vitro assays.
439
440 **PBMC culture**
441 PBMCs were cultured for 15 hrs or 7 days in RPMI (GIBCO) supplemented with 10% (v/v) heat
442 inactivated FBS, penicillin/streptomycin (100 U/mL), L-glutamine (2 mM), sodium pyruvate (1
443 mM), nonessential amino acids (0.1 mM), HEPES buffer (10 mM) and 2-mercaptoethanol (50 μM)
444 (from GIBCO or Sigma Aldrich) at 37°C 5% CO2 in 96 well plates in the presence of IL2 (GIBCO
445 100 IU/mL or Roche 1 ng/mL). Additional conditions included 1 ng/mL TGFβ (GIBCO). 2 μM 5-
446 A-RU was added directly to 50 μM methylglyoxal to form 5-OP-RU for in vitro stimulation assays.
447 5-A-RU was synthesized as previously described(Li et al., 2018), resuspended in 200 μM
448 aliquots, cryopreserved, and thawed as needed. αCD3/CD28 beads (Gibco) were incubated
449 with PBMCs at a 1:2 bead:cell ratio.
450
451 **Flow cytometry**
452 Cells were washed once in FACS buffer then incubated with Fc Receptor antibodies
453 (eBioscience; Fisher catalog # 14-1961-73) for 15 minutes at room temperature prior to staining.
454 Extracellular staining was performed at room temperature for 15 minutes in 50 μL FACS buffer
455 (eBioscience) while intracellular staining was performed after 2 hours of incubation in Brefeldin
456 A at 37°C followed by 45 minutes of incubation in 50 μL Permeabilization/Fixation buffer
457 (eBioscience), for 1 hour in 50 μl Permeabilization Buffer (eBioscience) at 4°C
458
459 The flow cytometric gating strategy to identify MAIT cells using MR1-5-OP-RU tetramers
460 generated by the NIH tetramer core facility(Corbett et al., 2014; Li et al., 2018) is summarized in

461 Supplementary Fig. 1. The % of MAIT cells of total $CD3^+$ cells and the absolute number of cells
462 sorted per condition are presented in Supplementary Tables 1a and b.
463
464 Cell staining was performed using the following fluorophore-conjugated antibodies (purchased
465 from BD, eBioscience or Biolegend; clones in parentheses): GZMB (GB11), ki67 (20Raj1), FoxP3
466 (PHC101), IFNγ (4S.BS3), TNFα (MAb11), CD25 (BC96), OX40 (ACT35), CD161 (DX12), CD3
467 (UCHT1), CD8 (SK1), CD4 (SK3), EOMES (WD1928), CTLA4 (BNI3), GZMA (CB9), GZMK
468 (GM26E7), IL7R (HIL-7R-M21), CD69 (FN50), ICOS (ISA-3), FAS (DX2), LAG3 (11C3C65) and PD1
469 (EH12.2H7), CCR7 (3D12).
470
471 **Flow-assisted cell sorting and flow cytometric analysis**
472 Stained cells were sorted on a BD Aria sorter or analyzed on a BD Fortessa analyzer. Flow
473 cytometry plots and analysis were performed using FCS Express version 7 (De Novo Software,
474 Pasadena, CA). Graphs and statistical analysis of flow cytometry data were generated using
475 Prism version 11 software (Graphpad Software, San Diego, CA).
476
477 **Cell barcoding and scRNA-seq library preparation**
478 The FACS-sorted live-cell suspensions were encapsulated in microfluidic droplets using a
479 Chromium instrument (10X genomics) and reagents provided in Single Cell 3' Reagent Kit (v3).
480 The barcoded-cDNA libraries were prepared according to the manual (CG00183 Rev B). The
481 viability of cells (stained with 0.2% (w/v) Trypan Blue) prior to loading onto the Chromium
482 instrument was 80-98%. Each sample was encapsulated at a final dilution of ~100 cells/μl.
483 Following the reverse transcription step the emulsion droplets were broken, barcoded-cDNA
484 purified with DynaBeads and amplified by 12-cycles of PCR: 98℃ for 180 s, 12x (98℃ for 15 s,
485 67˚C for 20 s, 72℃ for 60 s), and 72℃ for 60 s. The 50 ng of PCR-amplified barcoded-cDNA was

486 fragmented with the reagents provided in the kit, purified with SPRI beads and resulting DNA
487 library was ligated to the sequencing adapter followed by indexing PCR: 98℃ for 45 s; 14x (98℃
488 for 20 s, 54℃ for 30 s, 72℃ for 20 s), and 72℃ for 60 s. The final DNA library was double-size
489 purified (0.6–0.8X) with SPRI beads and sequenced on Illumina Nova-Seq platform (R1 – 26
490 cycles, i7 – 8 cycles, R2 – 70 cycles or higher) at depth of 220 million reads per sample.
491

492 **Single cell RNA-seq analysis**

493 Pre-processing of scRNA-seq fastq files was conducted using cellranger v3.0.2 (10x genomics).
494 scRNA-seq reads were aligned to the hg19 reference genome (ref-version 3.0.0), and the count
495 matrix of cell barcodes by genes used for downstream analysis was generated using the
496 cellranger count function with parameter –expect-cells=3000. The raw count matrix for each
497 sample was obtained from the cellranger count filter_matrix output. Briefly, for each sample,
498 cellranger plots the total UMI count against the cell barcode rank in decreasing order of total
499 counts, and filters cell barcodes out of the resulting count matrix based on the inflection point of
500 the plot. This step minimizes the number of empty droplets that are included in downstream
501 analyses. We created an initial count matrix combining all samples from all patients. Following
502 count matrix generation, cells with > 20% of transcripts derived from mitochondrial genes were
503 considered apoptotic, and were thus excluded. Following this step, all mitochondrial genes were
504 filtered out of the count matrix. Ribosomal genes and the noncoding RNAs NEAT1 and MALAT1
505 were excluded due to prior reports of strong influence on downstream clustering. Genes with
506 mean raw count < 3.0 were removed from the analysis, and we restricted to KLRB1+ cells,
507 resulting in a final count matrix of 76845 cells and xxx genes for downstream analysis. We used
508 Seurat v2.3.4 to perform standard library size and log normalization. The mean library size was
509 6680 transcripts per cell.

510 To examine potential batch effects in the data, we computed the prevalence of each cluster out
511 of all cells in each sample, followed by a centered log-ratio (CLR) transformation for
512 compositional data and PCA. This analysis demonstrated that samples clustered by timepoint,
513 not batch (i.e. donor). Differential expression analyses were conducted using the FindMarkers()
514 function in Seurat using a Wilcoxon test. Specifically, we compared each cluster to all other
515 clusters (one vs all), and genes were considered signature genes for a cluster if the log fold
516 change was greater than 0 and FDR P <= 0.05.
517

514

515 **References**

516

517 Bhattacharyya, A., Hanafi, L.A., Sheih, A., Golob, J.L., Srinivasan, S., Boeckh, M.J., Pergam,
518 S.A., Mahmood, S., Baker, K.K., Gooley, T.A.*, et al.* (2018). Graft-Derived Reconstitution of
519 Mucosal-Associated Invariant T Cells after Allogeneic Hematopoietic Cell Transplantation. Biol
520 Blood Marrow Transplant *24*, 242-251.
521 Boulouis, C., Sia, W.R., Gulam, M.Y., Teo, J.Q.M., Png, Y.T., Phan, T.K., Mak, J.Y.W., Fairlie,
522 D.P., Poon, I.K.H., Koh, T.H.*, et al.* (2020). Human MAIT cell cytolytic effector proteins
523 synergize to overcome carbapenem resistance in Escherichia coli. PLoS Biol *18*, e3000644.
524 Corbett, A.J., Eckle, S.B., Birkinshaw, R.W., Liu, L., Patel, O., Mahony, J., Chen, Z.,
525 Reantragoon, R., Meehan, B., Cao, H.*, et al.* (2014). T-cell activation by transitory neo-antigens
526 derived from distinct microbial pathways. Nature *509*, 361-365.
527 Coulter, F., Parrish, A., Manning, D., Kampmann, B., Mendy, J., Garand, M., Lewinsohn, D.M.,
528 Riley, E.M., and Sutherland, J.S. (2017). IL-17 Production from T Helper 17, Mucosal-
529 Associated Invariant T, and gammadelta Cells in Tuberculosis Infection and Disease. Front
530 Immunol *8*, 1252.
531 Dias, J., Boulouis, C., Gorin, J.B., van den Biggelaar, R., Lal, K.G., Gibbs, A., Loh, L., Gulam,
532 M.Y., Sia, W.R., Bari, S.*, et al.* (2018). The CD4(-)CD8(-) MAIT cell subpopulation is a
533 functionally distinct subset developmentally related to the main CD8(+) MAIT cell pool. Proc Natl
534 Acad Sci U S A *115*, E11513-E11522.
535 Dias, J., Leeansyah, E., and Sandberg, J.K. (2017). Multiple layers of heterogeneity and subset
536 diversity in human MAIT cell responses to distinct microorganisms and to innate cytokines. Proc
537 Natl Acad Sci U S A *114*, E5434-E5443.
538 Duan, M., Goswami, S., Shi, J.Y., Wu, L.J., Wang, X.Y., Ma, J.Q., Zhang, Z., Shi, Y., Ma, L.J.,
539 Zhang, S.*, et al.* (2019). Activated and Exhausted MAIT Cells Foster Disease Progression and
540 Indicate Poor Outcome in Hepatocellular Carcinoma. Clin Cancer Res *25*, 3304-3316.
541 Dusseaux, M., Martin, E., Serriari, N., Peguillet, I., Premel, V., Louis, D., Milder, M., Le Bourhis,
542 L., Soudais, C., Treiner, E., and Lantz, O. (2011). Human MAIT cells are xenobiotic-resistant,
543 tissue-targeted, CD161hi IL-17-secreting T cells. Blood *117*, 1250-1259.
544 Estevez, O., Anibarro, L., Garet, E., Martinez, A., Pena, A., Barcia, L., Peleteiro, M., and
545 Gonzalez-Fernandez, A. (2020). Multi-parameter flow cytometry immunophenotyping
546 distinguishes different stages of tuberculosis infection. J Infect.
547 Fink, P.J., and Hendricks, D.W. (2011). Post-thymic maturation: young T cells assert their
548 individuality. Nat Rev Immunol *11*, 544-549.
549 Gherardin, N.A., Loh, L., Admojo, L., Davenport, A.J., Richardson, K., Rogers, A., Darcy, P.K.,
550 Jenkins, M.R., Prince, H.M., Harrison, S.J.*, et al.* (2018a). Enumeration, functional responses
551 and cytotoxic capacity of MAIT cells in newly diagnosed and relapsed multiple myeloma. Sci
552 Rep *8*, 4159.
553 Gherardin, N.A., Souter, M.N., Koay, H.F., Mangas, K.M., Seemann, T., Stinear, T.P., Eckle,
554 S.B., Berzins, S.P., d'Udekem, Y., Konstantinov, I.E.*, et al.* (2018b). Human blood MAIT cell
555 subsets defined using MR1 tetramers. Immunol Cell Biol *96*, 507-525.
556 Godfrey, D.I., Koay, H.F., McCluskey, J., and Gherardin, N.A. (2019). The biology and
557 functional importance of MAIT cells. Nat Immunol.

558 Harriff, M.J., McMurtrey, C., Froyd, C.A., Jin, H., Cansler, M., Null, M., Worley, A., Meermeier,
559 E.W., Swarbrick, G., Nilsen, A.*, et al.* (2018). MR1 displays the microbial metabolome driving
560 selective MR1-restricted T cell receptor usage. Sci Immunol *3*.
561 Hengst, J., Strunz, B., Deterding, K., Ljunggren, H.G., Leeansyah, E., Manns, M.P., Cornberg,
562 M., Sandberg, J.K., Wedemeyer, H., and Bjorkstrom, N.K. (2016). Nonreversible MAIT cell-
563 dysfunction in chronic hepatitis C virus infection despite successful interferon-free therapy. Eur J
564 Immunol *46*, 2204-2210.
565 Hoffmann, P., Eder, R., Kunz-Schughart, L.A., Andreesen, R., and Edinger, M. (2004). Large-
566 scale in vitro expansion of polyclonal human CD4(+)CD25high regulatory T cells. Blood *104*,
567 895-903.
568 Jahreis, S., Bottcher, S., Hartung, S., Rachow, T., Rummler, S., Dietl, A.M., Haas, H., Walther,
569 G., Hochhaus, A., and von Lilienfeld-Toal, M. (2018). Human MAIT cells are rapidly activated by
570 Aspergillus spp. in an APC-dependent manner. Eur J Immunol *48*, 1698-1706.
571 Jiang, J., Cao, Z., Qu, J., Liu, H., Han, H., and Cheng, X. (2020). PD-1-expressing MAIT cells
572 from patients with tuberculosis exhibit elevated production of CXCL13. Scand J Immunol *91*,
573 e12858.
574 Kelly, J., Minoda, Y., Meredith, T., Cameron, G., Philipp, M.S., Pellicci, D.G., Corbett, A.J.,
575 Kurts, C., Gray, D.H., Godfrey, D.I.*, et al.* (2019). Chronically stimulated human MAIT cells are
576 unexpectedly potent IL-13 producers. Immunol Cell Biol *97*, 689-699.
577 Koay, H.F., Su, S., Amann-Zalcenstein, D., Daley, S.R., Comerford, I., Miosge, L., Whyte, C.E.,
578 Konstantinov, I.E., d'Udekem, Y., Baldwin, T.*, et al.* (2019). A divergent transcriptional
579 landscape underpins the development and functional branching of MAIT cells. Sci Immunol *4*.
580 Kurioka, A., Jahun, A.S., Hannaway, R.F., Walker, L.J., Fergusson, J.R., Sverremark-Ekstrom,
581 E., Corbett, A.J., Ussher, J.E., Willberg, C.B., and Klenerman, P. (2017). Shared and Distinct
582 Phenotypes and Functions of Human CD161++ Valpha7.2+ T Cell Subsets. Front Immunol *8*,
583 1031.
584 Lamichhane, R., Galvin, H., Hannaway, R.F., de la Harpe, S.M., Munro, F., Tyndall, J.D.,
585 Vernall, A.J., McCall, J.L., Husain, M., and Ussher, J.E. (2020). Type I interferons are important
586 co-stimulatory signals during T cell receptor mediated human MAIT cell activation. Eur J
587 Immunol *50*, 178-191.
588 Lamichhane, R., Schneider, M., de la Harpe, S.M., Harrop, T.W.R., Hannaway, R.F., Dearden,
589 P.K., Kirman, J.R., Tyndall, J.D.A., Vernall, A.J., and Ussher, J.E. (2019). TCR- or Cytokine-
590 Activated CD8(+) Mucosal-Associated Invariant T Cells Are Rapid Polyfunctional Effectors That
591 Can Coordinate Immune Responses. Cell Rep *28*, 3061-3076 e3065.
592 Leeansyah, E., Ganesh, A., Quigley, M.F., Sonnerborg, A., Andersson, J., Hunt, P.W.,
593 Somsouk, M., Deeks, S.G., Martin, J.N., Moll, M.*, et al.* (2013). Activation, exhaustion, and
594 persistent decline of the antimicrobial MR1-restricted MAIT-cell population in chronic HIV-1
595 infection. Blood *121*, 1124-1135.
596 Leeansyah, E., Svard, J., Dias, J., Buggert, M., Nystrom, J., Quigley, M.F., Moll, M.,
597 Sonnerborg, A., Nowak, P., and Sandberg, J.K. (2015). Arming of MAIT Cell Cytolytic
598 Antimicrobial Activity Is Induced by IL-7 and Defective in HIV-1 Infection. PLoS Pathog *11*,
599 e1005072.
600 Legoux, F., Bellet, D., Daviaud, C., El Morr, Y., Darbois, A., Niort, K., Procopio, E., Salou, M.,
601 Gilet, J., Ryffel, B.*, et al.* (2019). Microbial metabolites control the thymic development of
602 mucosal-associated invariant T cells. Science *366*, 494-499.
603 Leng, T., Akther, H.D., Hackstein, C.P., Powell, K., King, T., Friedrich, M., Christoforidou, Z.,
604 McCuaig, S., Neyazi, M., Arancibia-Carcamo, C.V.*, et al.* (2019). TCR and Inflammatory Signals
605 Tune Human MAIT Cells to Exert Specific Tissue Repair and Effector Functions. Cell Rep *28*,
606 3077-3091 e3075.

607 Li, K., Vorkas, C.K., Chaudhry, A., Bell, D.L., Willis, R.A., Rudensky, A., Altman, J.D., Glickman,
608 M.S., and Aube, J. (2018). Synthesis, stabilization, and characterization of the MR1 ligand
609 precursor 5-amino-6-D-ribitylaminouracil (5-A-RU). PLoS One *13*, e0191837.
610 Ling, L., Lin, Y., Zheng, W., Hong, S., Tang, X., Zhao, P., Li, M., Ni, J., Li, C., Wang, L., and
611 Jiang, Y. (2016). Circulating and tumor-infiltrating mucosal associated invariant T (MAIT) cells in
612 colorectal cancer patients. Sci Rep *6*, 20358.
613 Liston, A., Nutsch, K.M., Farr, A.G., Lund, J.M., Rasmussen, J.P., Koni, P.A., and Rudensky,
614 A.Y. (2008). Differentiation of regulatory Foxp3+ T cells in the thymic cortex. Proc Natl Acad Sci
615 U S A *105*, 11903-11908.
616 Maruhashi, T., Okazaki, I.M., Sugiura, D., Takahashi, S., Maeda, T.K., Shimizu, K., and
617 Okazaki, T. (2018). LAG-3 inhibits the activation of CD4(+) T cells that recognize stable pMHCII
618 through its conformation-dependent recognition of pMHCII. Nat Immunol *19*, 1415-1426.
619 Rouxel, O., Da Silva, J., Beaudoin, L., Nel, I., Tard, C., Cagninacci, L., Kiaf, B., Oshima, M.,
620 Diedisheim, M., Salou, M.*, et al.* (2017). Cytotoxic and regulatory roles of mucosal-associated
621 invariant T cells in type 1 diabetes. Nat Immunol *18*, 1321-1331.
622 Saeidi, A., Tien Tien, V.L., Al-Batran, R., Al-Darraji, H.A., Tan, H.Y., Yong, Y.K.,
623 Ponnampalavanar, S., Barathan, M., Rukumani, D.V., Ansari, A.W.*, et al.* (2015). Attrition of
624 TCR Va7.2+CD161++ MAIT cells in HIV-tuberculosis co-infection is associated with elevated
625 levels of PD-1 expression. PLoS ONE *10*, 1-14.
626 Sasson, S.C., Zaunders, J.J., Nahar, K., Munier, C.M.L., Fairfax, B.P., Olsson-Brown, A., Jolly,
627 C., Read, S.A., Ahlenstiel, G., Palendira, U.*, et al.* (2020). Mucosal-associated invariant T
628 (MAIT) cells are activated in the gastrointestinal tissue of patients with combination ipilimumab
629 and nivolumab therapy-related colitis in a pathology distinct from ulcerative colitis. Clin Exp
630 Immunol.
631 Seshadri, C., Thuong, N.T., Mai, N.T., Bang, N.D., Chau, T.T., Lewinsohn, D.M., Thwaites,
632 G.E., Dunstan, S.J., and Hawn, T.R. (2017). A polymorphism in human MR1 is associated with
633 mRNA expression and susceptibility to tuberculosis. Genes Immun *18*, 8-14.
634 Shaler, C.R., Choi, J., Rudak, P.T., Memarnejadian, A., Szabo, P.A., Tun-Abraham, M.E.,
635 Rossjohn, J., Corbett, A.J., McCluskey, J., McCormick, J.K.*, et al.* (2017). MAIT cells launch a
636 rapid, robust and distinct hyperinflammatory response to bacterial superantigens and quickly
637 acquire an anergic phenotype that impedes their cognate antimicrobial function: Defining a
638 novel mechanism of superantigen-induced immunopathology and immunosuppression. PLoS
639 Biol *15*, e2001930.
640 Slichter, C.K., McDavid, A., Miller, H.W., Finak, G., Seymour, B.J., McNevin, J.P., Diaz, G.,
641 Czartoski, J.L., McElrath, M.J., Gottardo, R., and Prlic, M. (2016). Distinct activation thresholds
642 of human conventional and innate-like memory T cells. JCI Insight *1*.
643 Suliman, S., Murphy, M., Musvosvi, M., Gela, A., Meermeier, E.W., Geldenhuys, H., Hopley, C.,
644 Toefy, A., Bilek, N., Veldsman, A.*, et al.* (2019). MR1-Independent Activation of Human
645 Mucosal-Associated Invariant T Cells by Mycobacteria. J Immunol *203*, 2917-2927.
646 Treiner, E., Duban, L., Bahram, S., Radosavljevic, M., Wanner, V., Tilloy, F., Affaticati, P.,
647 Gilfillan, S., and Lantz, O. (2003). Selection of evolutionarily conserved mucosal-associated
648 invariant T cells by MR1. Nature *422*, 164-169.
649 Trickett, A., and Kwan, Y.L. (2003). T cell stimulation and expansion using anti-CD3/CD28
650 beads. J Immunol Methods *275*, 251-255.
651 Trinchieri, G. (2010). Type I interferon: friend or foe? J Exp Med *207*, 2053-2063.
652 van Wilgenburg, B., Scherwitzl, I., Hutchinson, E.C., Leng, T., Kurioka, A., Kulicke, C., de Lara,
653 C., Cole, S., Vasanawathana, S., Limpitikul, W.*, et al.* (2016). MAIT cells are activated during
654 human viral infections. Nat Commun *7*, 11653.

655 Venken, K., Favreau, M., Gaublomme, D., Menu, E., Vanderkerken, K., and Elewaut, D. (2018).
656 Checkpoint inhibition in the treatment of multiple myeloma: A way to boost innate-like T cell anti-
657 tumor function? Mol Immunol *101*, 521-526.
658 Vorkas, C.K., Wipperman, M.F., Li, K., Bean, J., Bhattarai, S.K., Adamow, M., Wong, P., Aube,
659 J., Juste, M.A.J., Bucci, V.*, et al.* (2018). Mucosal-associated invariant and gammadelta T cell
660 subsets respond to initial Mycobacterium tuberculosis infection. JCI Insight *3*.
661 Welsh, R.M., Bahl, K., Marshall, H.D., and Urban, S.L. (2012). Type 1 interferons and antiviral
662 CD8 T-cell responses. PLoS Pathog *8*, e1002352.
663 Yamaguchi, T., Wing, J.B., and Sakaguchi, S. (2011). Two modes of immune suppression by
664 Foxp3(+) regulatory T cells under inflammatory or non-inflammatory conditions. Semin Immunol
665 *23*, 424-430.
666 Yong, Y.K., Saeidi, A., Tan, H.Y., Rosmawati, M., Enstrom, P.F., Batran, R.A., Vasuki, V.,
667 Chattopadhyay, I., Murugesan, A., Vignesh, R.*, et al.* (2018). Hyper-Expression of PD-1 Is
668 Associated with the Levels of Exhausted and Dysfunctional Phenotypes of Circulating
669 CD161(++)TCR iValpha7.2(+) Mucosal-Associated Invariant T Cells in Chronic Hepatitis B Virus
670 Infection. Front Immunol *9*, 472.
671

672

Fig. 1

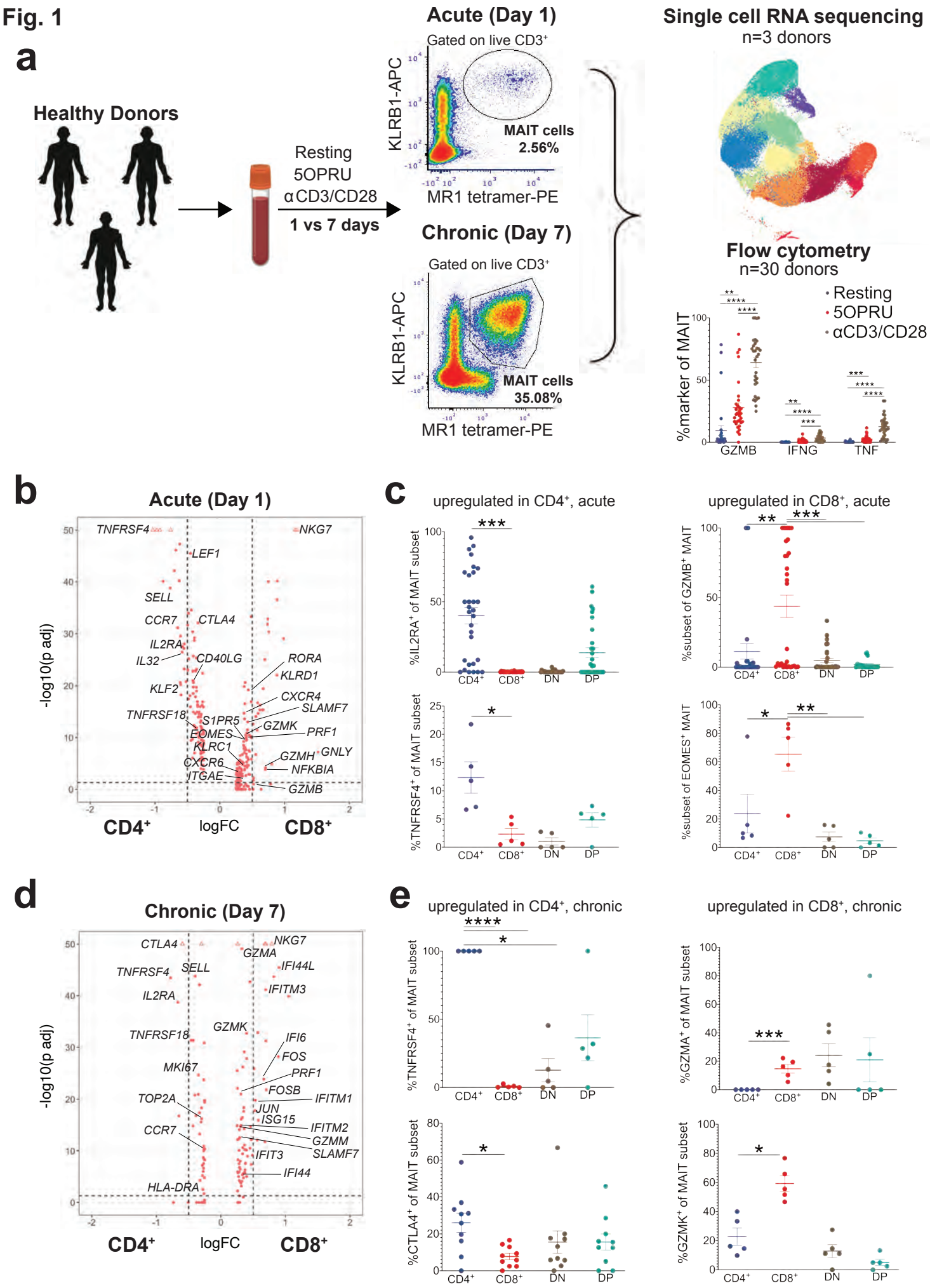
a
Healthy Donors
Resting
5OPRU
αCD3/CD28
1 vs 7 days
Acute (Day 1)
Gated on live CD3+
KLRB1-APC
MAIT cells
2.56%
MR1 tetramer-PE
Chronic (Day 7)
Gated on live CD3+
KLRB1-APC
MAIT cells
35.08%
MR1 tetramer-PE
Single cell RNA sequencing
n=3 donors
Flow cytometry
n=30 donors
Resting
5OPRU
αCD3/CD28
%marker of MAIT
GZMB
IFNG
TNF
b
Acute (Day 1)
-log10(p adj)
TNFRSF4
NKG7
LEF1
SELL
CCR7
CTLA4
IL2RA
IL32
CD40LG
RORA
KLRD1
KLF2
CXCR4
SLAMF7
TNFRSF18
S1PR5
GZMK
EOMES
PRF1
KLRC1
GZMH
GNLY
CXCR6
NFKBIA
ITGAE
GZMB
CD4+
logFC
CD8+
c
upregulated in CD4+, acute
%IL2RA+ of MAIT subset
%TNFRSF4+ of MAIT subset
upregulated in CD8+, acute
%subset of GZMB+ MAIT
%subset of EOMES+ MAIT
CD4+
CD8+
DN
DP
d
Chronic (Day 7)
-log10(p adj)
CTLA4
NKG7
GZMA
TNFRSF4
SELL
IFI44L
IL2RA
IFITM3
GZMK
TNFRSF18
IFI6
FOS
MKI67
PRF1
FOSB
TOP2A
IFITM1
JUN
ISG15
CCR7
IFITM2
GZMM
SLAMF7
IFIT3
IFI44
HLA-DRA
CD4+
logFC
CD8+
e
upregulated in CD4+, chronic
%TNFRSF4+ of MAIT subset
%CTLA4+ of MAIT subset
upregulated in CD8+, chronic
%GZMA+ of MAIT subset
%GZMK+ of MAIT subset
CD4+
CD8+
DN
DP

658

659 **Figure 1. MAIT cell CD4 or CD8 expression are associated with distinct transcriptional**

660 **signatures**

661

662 **(a)** Experimental schematic of the MAIT cell in vitro activation assay used for single cell RNA

663 sequencing (scRNA-seq) and flow cytometric analyses. A total of 30 healthy donor PBMCs were

664 assayed by flow cytometry after 15 hrs (D1; acute activation) or 7 days (D7; chronic activation)

665 of incubation under resting, 5OPRU or αCD3/CD28 conditions. A subset of three of these donors

666 underwent flow cytometry-assisted cell sorting (FACS) for scRNA-seq under the same

667 conditions. All conditions included IL2 and a subset of D7 conditions also included TGFβ. **(b)**

668 Differentially expressed genes in $CD8^+$ (+ log FC; log fold change) or $CD4^+$ MAIT cells (- log FC)

669 after 15 hours of incubation in the resting condition. y axis: log FDR-adjusted p value with a

670 significance level of FDR < 0.05. **(c)** Mean% +/- SEM of CD25, OX40, GZMB, and EOMES

671 staining in $CD4^+$, $CD8^+$, DN or DP MAIT cell subsets measured by flow cytometry in the same

672 condition as (b). Data representative of 3 independent experiments. n=5-30 donors. **(d)**

673 Differentially expressed genes in $CD8^+$ or $CD4^+$ MAIT cells after 7 days of incubation in the resting

674 condition. Same axes as (b). **(e)** Mean% +/- SEM of OX40, CTLA4, GZMA, and GZMK staining

675 in MAIT cell subsets measured by flow cytometry in the same condition as (d). Data

676 representative of 2 independent experiments. n=5-10 donors. Flow cytometric statistical

677 comparisons were made by unpaired t-test. *p<0.05 **p<0.005 *** p<0.0005 ****p<0.0001;

678 GZMB: granzyme B; GZMA: granzyme A; GZMK: granzyme K; DN: double-negative ($CD4^-CD8$);

679 DP: double-positive ($CD4^+CD8^+$)

680

681

Fig. 2

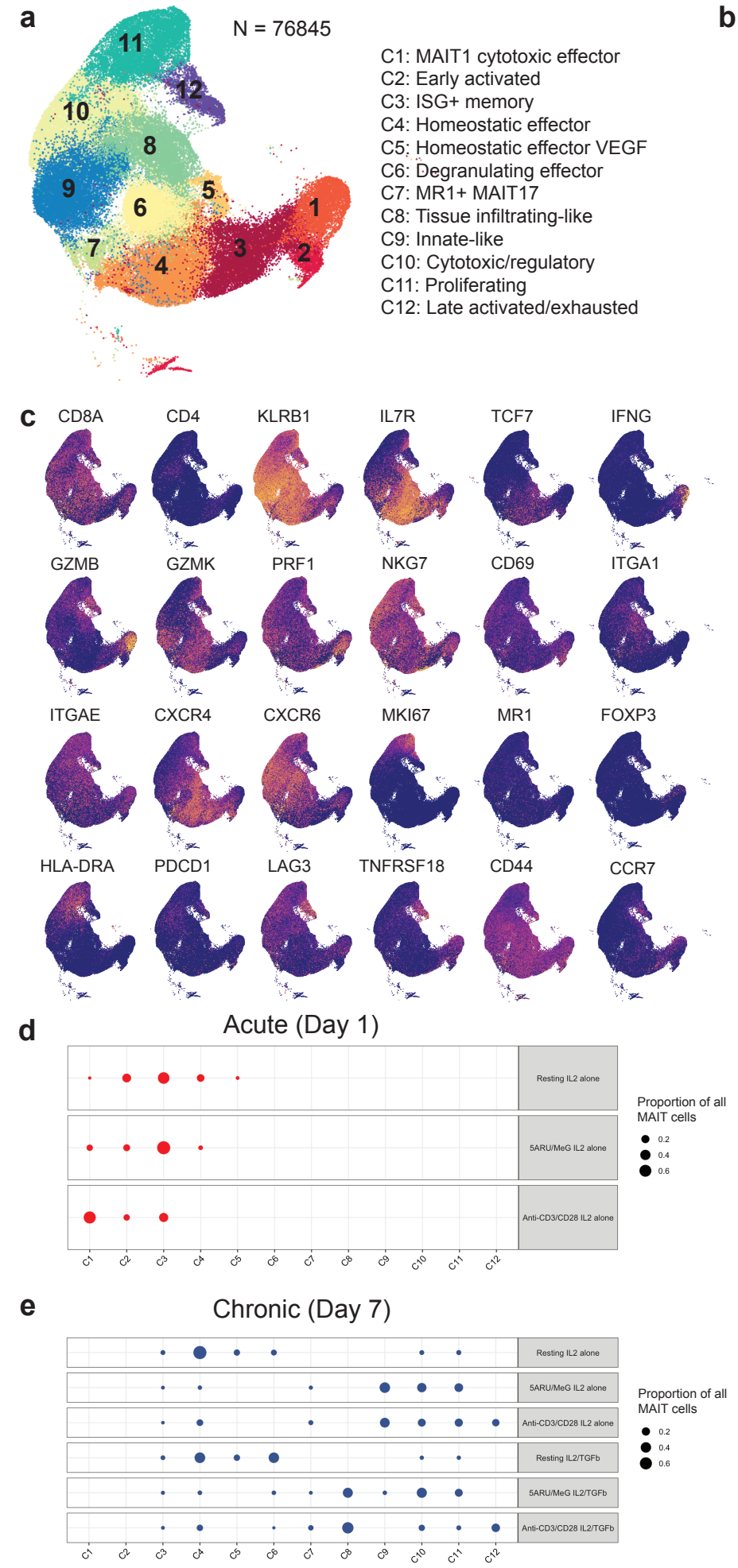
a
N = 76845
C1: MAIT1 cytotoxic effector
C2: Early activated
C3: ISG+ memory
C4: Homeostatic effector
C5: Homeostatic effector VEGF
C6: Degranulating effector
C7: MR1+ MAIT17
C8: Tissue infiltrating-like
C9: Innate-like
C10: Cytotoxic/regulatory
C11: Proliferating
C12: Late activated/exhausted
b
c
CD8A
CD4
KLRB1
IL7R
TCF7
IFNG
GZMB
GZMK
PRF1
NKG7
CD69
ITGA1
ITGAE
CXCR4
CXCR6
MKI67
MR1
FOXP3
HLA-DRA
PDCD1
LAG3
TNFRSF18
CD44
CCR7
d
Acute (Day 1)
Resting IL2 alone
5ARU/MeG IL2 alone
Anti-CD3/CD28 IL2 alone
Proportion of all MAIT cells
0.2
0.4
0.6
C1 C2 C3 C4 C5 C6 C7 C8 C9 C10 C11 C12
e
Chronic (Day 7)
Resting IL2 alone
5ARU/MeG IL2 alone
Anti-CD3/CD28 IL2 alone
Resting IL2/TGFb
5ARU/MeG IL2/TGFb
Anti-CD3/CD28 IL2/TGFb
Proportion of all MAIT cells
0.2
0.4
0.6
C1 C2 C3 C4 C5 C6 C7 C8 C9 C10 C11 C12
C3 C2 C1 C4 C5 C6 C10 C7 C9 C8 C11 C12

682

683 **Figure 2. Single cell transcriptional analysis defines heterogeneous MAIT cell activation**

684 **states.**

685

686 **(a)** Uniform manifold approximation and projection (UMAP) plot and Louvain clustering of cells

687 from all donors, timepoints and stimuli with ascribed names based on differentially expressed

688 gene sets in each cluster. **(b)** Heat map showing top 15 differentially expressed genes per cluster

689 after unsupervised hierarchical clustering. **(c)** UMAP plots of selected MAIT cell markers

690 demonstrating expression level across all clusters (blue=low expression to yellow=high

691 expression). **(d, e)** Dot plots demonstrating relative frequency of cells per condition in all donors.

692

Fig. 3

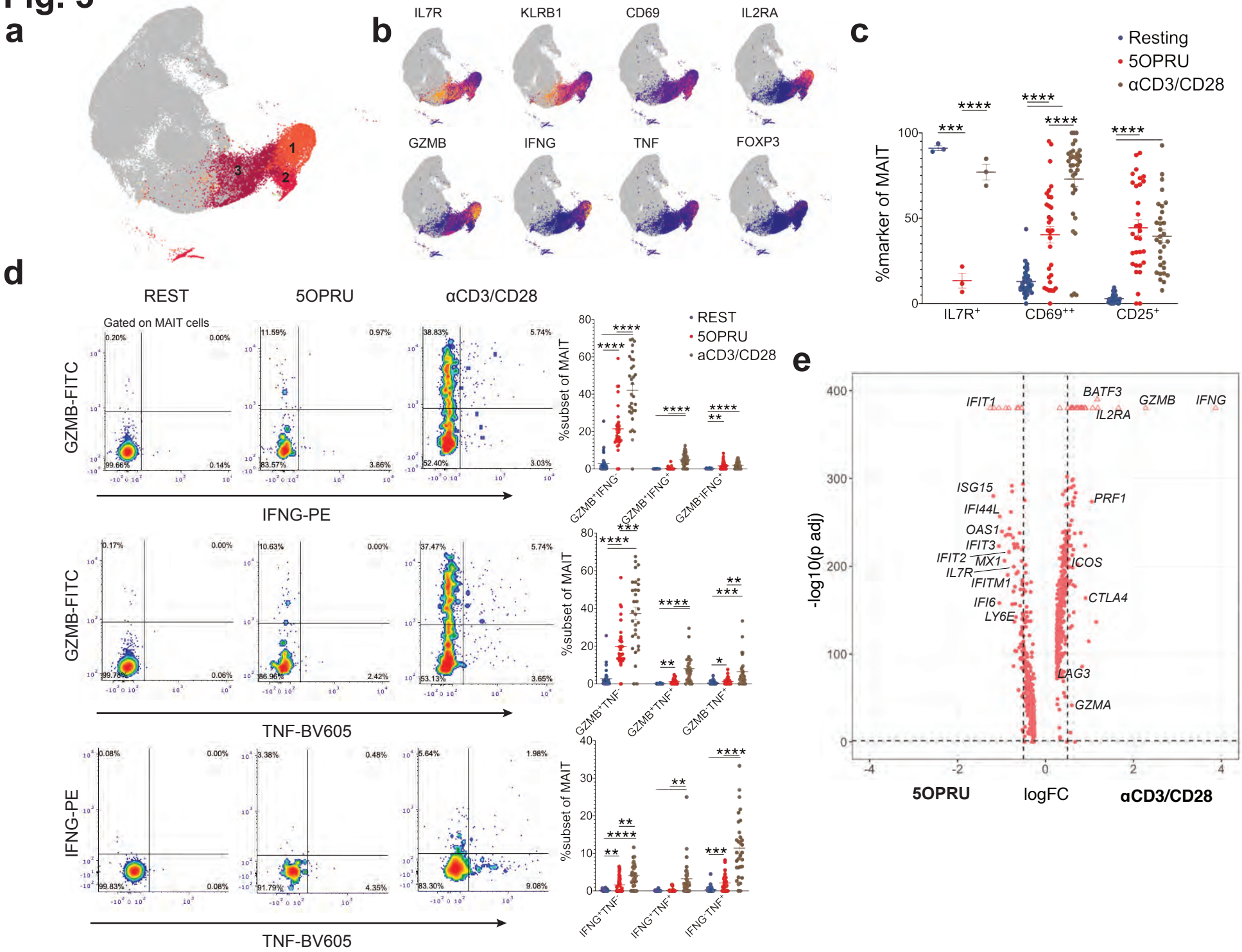
a
1
2
3
b
IL7R
KLRB1
CD69
IL2RA
GZMB
IFNG
TNF
FOXP3
c
Resting
5OPRU
αCD3/CD28
%marker of MAIT
IL7R+
CD69++
CD25+
d
REST
5OPRU
αCD3/CD28
Gated on MAIT cells
GZMB-FITC
IFNG-PE
TNF-BV605
%subset of MAIT
GZMB+IFNG+
GZMB+IFNG-
GZMB-IFNG-
GZMB+TNF+
GZMB+TNF-
GZMB-TNF-
IFNG+TNF+
IFNG+TNF-
IFNG-TNF-
e
-log10(p adj)
IFIT1
BATF3
GZMB
IFNG
IL2RA
ISG15
IFI44L
OAS1
IFIT3
IFIT2
MX1
IL7R
IFITM1
IFI6
LY6E
PRF1
ICOS
CTLA4
LAG3
GZMA
5OPRU
logFC
αCD3/CD28

693 **Figure 3. Acute MAIT cell activation induces a cytotoxic phenotype marked by GZMB,**
694 **IFNG, and TNF**
695
696 **(a)** UMAP plot highlighting clusters 1-3 enriched in day 1 (D1) incubation conditions. **(b)** UMAP
697 plots of selected MAIT cell marker expression levels at D1 (blue=low expression to yellow=high
698 expression). **(c)** Mean% +/- SEM of MAIT cell extracellular staining of activation markers
699 detected by flow cytometry after 15 hrs of incubation in three conditions: resting (blue), 5OPRU
700 (red), αCD3/CD28 (brown). Results are representative of 4 independent experiments: n=3-30
701 donors. **(d)** Representative flow cytometry density plots in one donor demonstrating GZMB,
702 TNFα and IFNγ co-staining (left) alongside cumulative plots (right) of mean% +/- SEM for each
703 co-staining condition in multiple donors. Results are representative of 4 independent
704 experiments. n=30 donors. **(e)** Differentially expressed genes in the αCD3/CD28 (+ log fold
705 change; log FC) or 5OPRU (- log FC) conditions at D1. y axis: log FDR-adjusted p value at
706 significance level of FDR $P < 0.05$. Flow cytometric statistical comparisons were made by
707 unpaired t-test. *p<0.05 **p<0.005 *** p<0.0005 ****p<0.0001; GZMB: granzyme B
708

Fig. 4

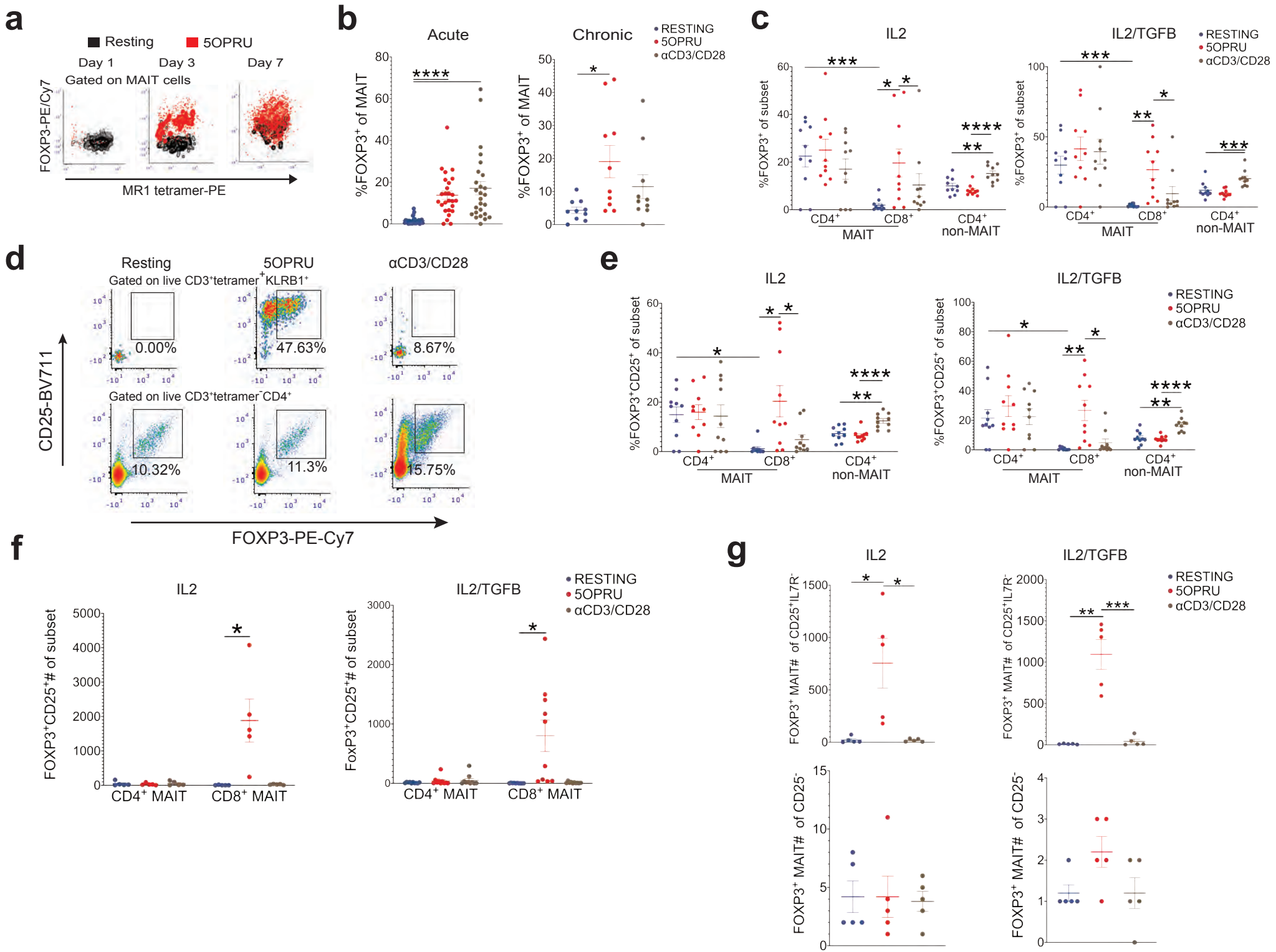
a
Resting
5OPRU
Day 1
Day 3
Day 7
Gated on MAIT cells
FOXP3-PE/Cy7
MR1 tetramer-PE
b
Acute
Chronic
RESTING
5OPRU
αCD3/CD28
%FOXP3+ of MAIT
c
IL2
IL2/TGFB
%FOXP3+ of subset
CD4+
CD8+
MAIT
CD4+ non-MAIT
d
Resting
5OPRU
αCD3/CD28
Gated on live CD3+tetramer+KLRB1+
Gated on live CD3+tetramer-CD4+
0.00%
47.63%
8.67%
10.32%
11.3%
15.75%
CD25-BV711
FOXP3-PE-Cy7
e
IL2
IL2/TGFB
%FOXP3+CD25+ of subset
f
IL2
IL2/TGFB
FOXP3+CD25+# of subset
FoxP3+CD25+# of subset
CD4+ MAIT
CD8+ MAIT
g
IL2
IL2/TGFB
FOXP3+ MAIT# of CD25+IL7R-
FOXP3+ MAIT# of CD25-

709 **Figure 4. MAIT cells upregulate FoxP3 during acute and chronic activation**

710

711 **(a)** Representative flow cytometry contour plots of MAIT cell FOXP3 intracellular staining in
712 resting or 5OPRU conditions after 1, 3, or 7 days of stimulation (black=resting; red=5OPRU). **(b)**
713 Mean% +/- SEM of intracellular MAIT cell FOXP3 staining after 1 (D1; acute) or 7 (D7; chronic)
714 days of incubation under resting (blue), 5OPRU (red), or αCD3/CD28 (brown) conditions. Data
715 representative of 3 independent experiments. n=10-26 donors. **(c)** Mean% +/- SEM of
716 intracellular FOXP3 staining in $CD4^+$ and $CD8^+$ MAIT cells compared to non-MAIT $CD4^+$ T cells
717 after 7 days of incubation in the same conditions as (b). **(d)** Representative flow cytometry
718 density plots from one donor demonstrating $FOXP3^+CD25^+$ MAIT cells (top row) or non-MAIT
719 $CD4^+$ T cells (bottom row) after 7 days of incubation in the same conditions as (b). **(e)** Mean%
720 +/- SEM of $FOXP3^+CD25^+$ $CD4^+$ or $CD8^+$ MAIT cells compared to non-MAIT $CD4^+$ T cells after 7
721 days in the same conditions as (b). Cytokine co-incubation conditions included IL2 (left) or
722 IL2/TGFβ (right). Representative of two independent experiments. n=10 donors. **(f)** Mean
723 absolute number +/- SEM of $FOXP3^+CD25^+$ $CD4^+$ or $CD8^+$ MAIT cells in the same incubation
724 conditions as (e). Representative of 1 independent experiment. n=5 donors. **(g)** Mean absolute
725 number +/- SEM of $FOXP3^+$ MAIT cells among $CD25^+IL7R^-$ MAIT cells or $CD25^-$ MAIT cells after
726 7 days in the same incubation conditions as (e).

727

Fig. 5

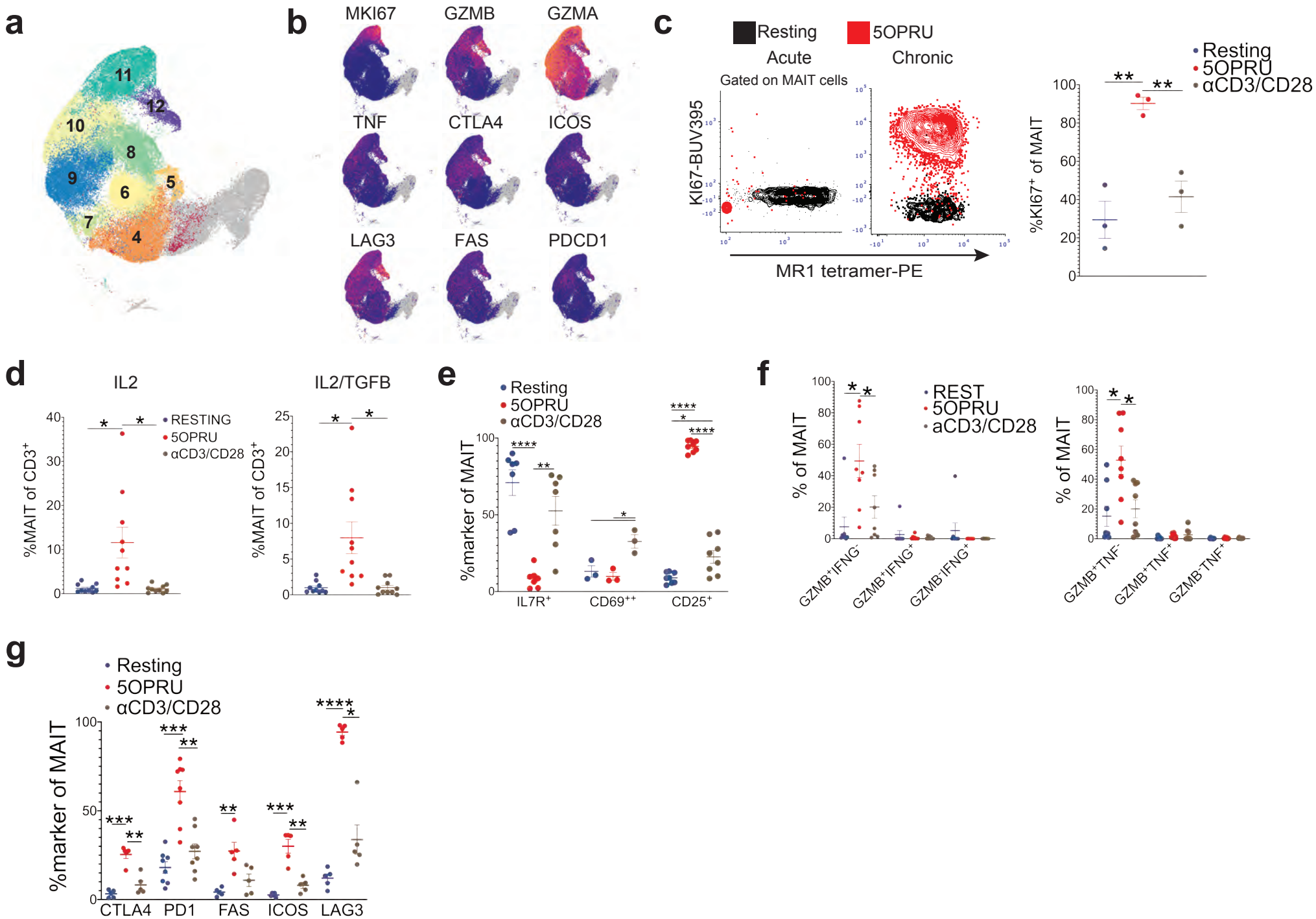
a
11
12
10
8
9
6
5
7
4
b
MKI67
GZMB
GZMA
TNF
CTLA4
ICOS
LAG3
FAS
PDCD1
c
Resting
5OPRU
Acute
Chronic
Gated on MAIT cells
KI67-BUV395
MR1 tetramer-PE
Resting
5OPRU
αCD3/CD28
%KI67+ of MAIT
d
IL2
IL2/TGFB
RESTING
5OPRU
αCD3/CD28
%MAIT of CD3+
e
Resting
5OPRU
αCD3/CD28
%marker of MAIT
IL7R+
CD69++
CD25+
f
REST
5OPRU
aCD3/CD28
% of MAIT
GZMB+IFNG-
GZMB+IFNG+
GZMB-IFNG+
GZMB+TNF-
GZMB+TNF+
GZMB-TNF+
g
Resting
5OPRU
αCD3/CD28
%marker of MAIT
CTLA4
PD1
FAS
ICOS
LAG3

728 **Figure 5. Chronic activation of MAIT cells expands homeostatic subpopulations while also**
729 **inducing proliferative, cytotoxic, immune regulatory and exhaustion phenotypes**
730
731 **(a)** UMAP highlighting clusters 4-12 defined by day 7 (D7) incubation conditions. **(b)** UMAP plots
732 of selected MAIT cell marker expression levels at D7 (blue=low expression to yellow= high
733 expression). **(c)** Representative flow cytometry contour plots (left) of intracellular ki67 staining
734 after 15 hours (D1; acute) or 7 days (D7; chronic) of incubation at rest (black) or with 5OPRU (red)
735 accompanied by cumulative data of mean% +/- SEM of MAIT cell ki67 staining after 7 days of
736 incubation under resting (blue), 5OPRU (red) or αCD3/CD28 (brown) conditions (right). Data is
737 representative of one independent experiment. n=3 donors. **(d)** Mean% +/- SEM of MAIT cells
738 among total T cells after 7 days of incubation in the same conditions as (c). Data is representative
739 of two independent experiments. n=10 donors. **(e)** Mean% +/- SEM of MAIT cell surface
740 activation markers after 7 days of incubation in the same conditions as (c). Data is representative
741 of two independent experiments. n=3-8 donors. **(f)** GZMB, IFNγ, and TNFα intracellular co-
742 staining demonstrating mean% +/- SEM of each subset after 7 days of incubation under the
743 same conditions as (c). Data is representative of two independent experiments. n=8 donors. **(g)**
744 Mean% +/- SEM of activation/exhaustion marker staining after 7 days of incubation under the
745 same conditions as (c). Data is representative of one independent experiment. n=5 donors.
746 Data representative of one independent experiment. n=3 donors. Flow cytometric statistical
747 comparisons were made by unpaired t-test. *$p<0.05$ **$p<0.005$ *** $p<0.0005$ ****$p<0.0001$;
748 GZMB: granzyme B
749

Fig. 6

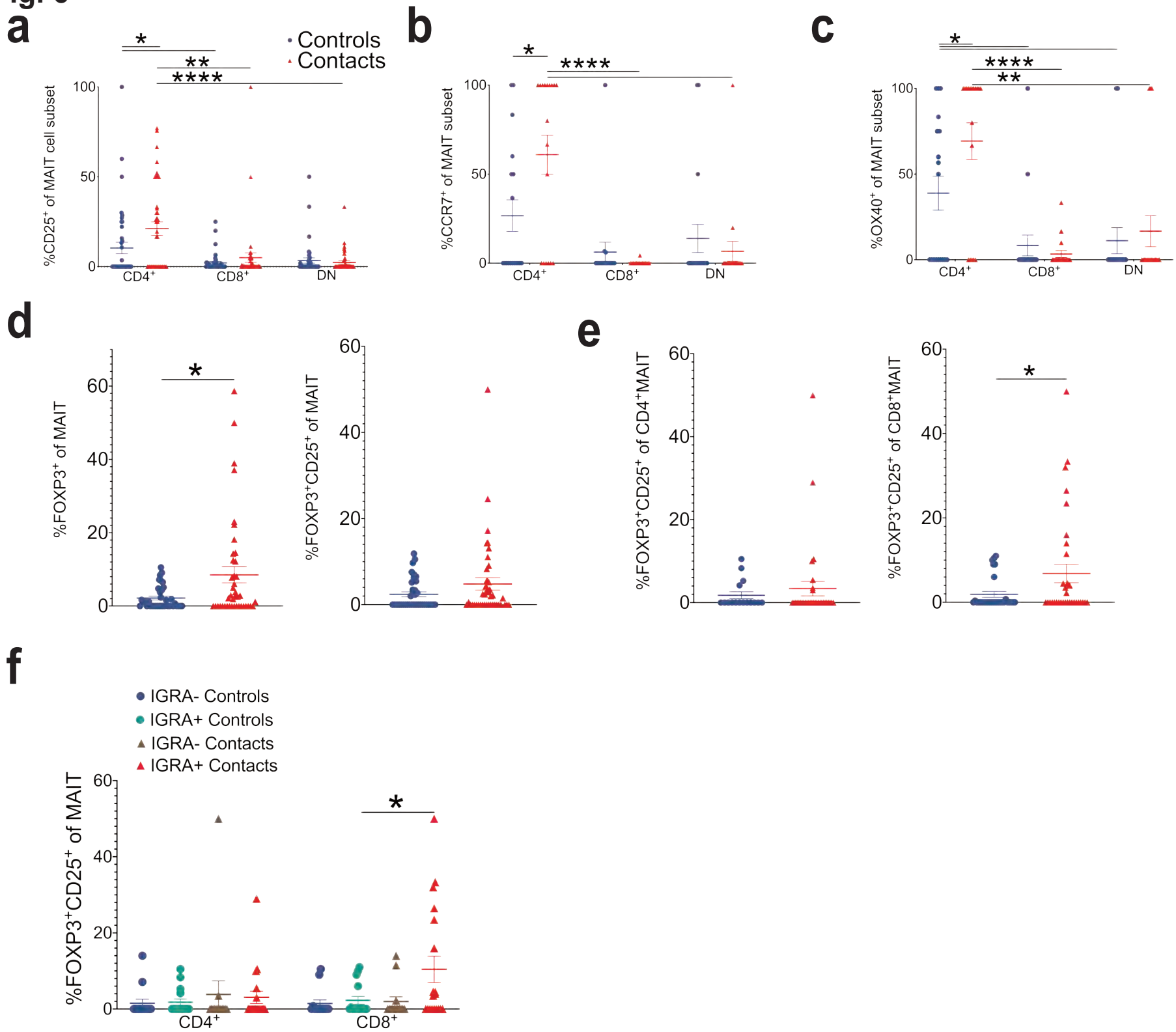
a
Controls
Contacts
%CD25+ of MAIT cell subset
CD4+
CD8+
DN
b
%CCR7+ of MAIT subset
c
%OX40+ of MAIT subset
d
%FOXP3+ of MAIT
%FOXP3+CD25+ of MAIT
e
%FOXP3+CD25+ of CD4+MAIT
%FOXP3+CD25+ of CD8+MAIT
f
IGRA- Controls
IGRA+ Controls
IGRA- Contacts
IGRA+ Contacts
%FOXP3+CD25+ of MAIT

750 **Figure 6. MAIT cell subsets differentially respond to acute and chronic activation** by
751 *Mycobacterium tuberculosis*
752
753 **(a-c)** Mean% +/- SEM of CD25 (a), CCR7 (b), and OX40 (c) staining of $CD4^+$, $CD8^+$ or DN MAIT
754 cell subsets in healthy household contacts of TB patients (red triangles) compared to healthy
755 unexposed community controls (blue circles). Same legend also applies to panels (d) and (e).
756 n=18-41 donors. **(d)** Mean% +/- SEM of $FOXP3^+$ (left) or $FOXP3^+CD25^+$ (right) MAIT cells. n=36-
757 42 donors. **(e)** Mean% +/- SEM of $FOXP3^+CD25^+$ $CD4^+$ (left) or $CD8^+$ MAIT cells (right) in the
758 same donors as (d). **(f)** Mean% +/- SEM of $FOXP3^+CD25^+$ $CD4^+$ or $C8^+$ MAIT cells stratified by
759 IGRA status in the same donors as (d). Flow cytometric statistical comparisons were made by
760 unpaired t-test. *$p<0.05$ **$p<0.005$ *** $p<0.0005$ ****$p<0.0001$; IGRA: *Mtb*-specific IFNγ release
761 assay.
762

Supplementary Figure 1

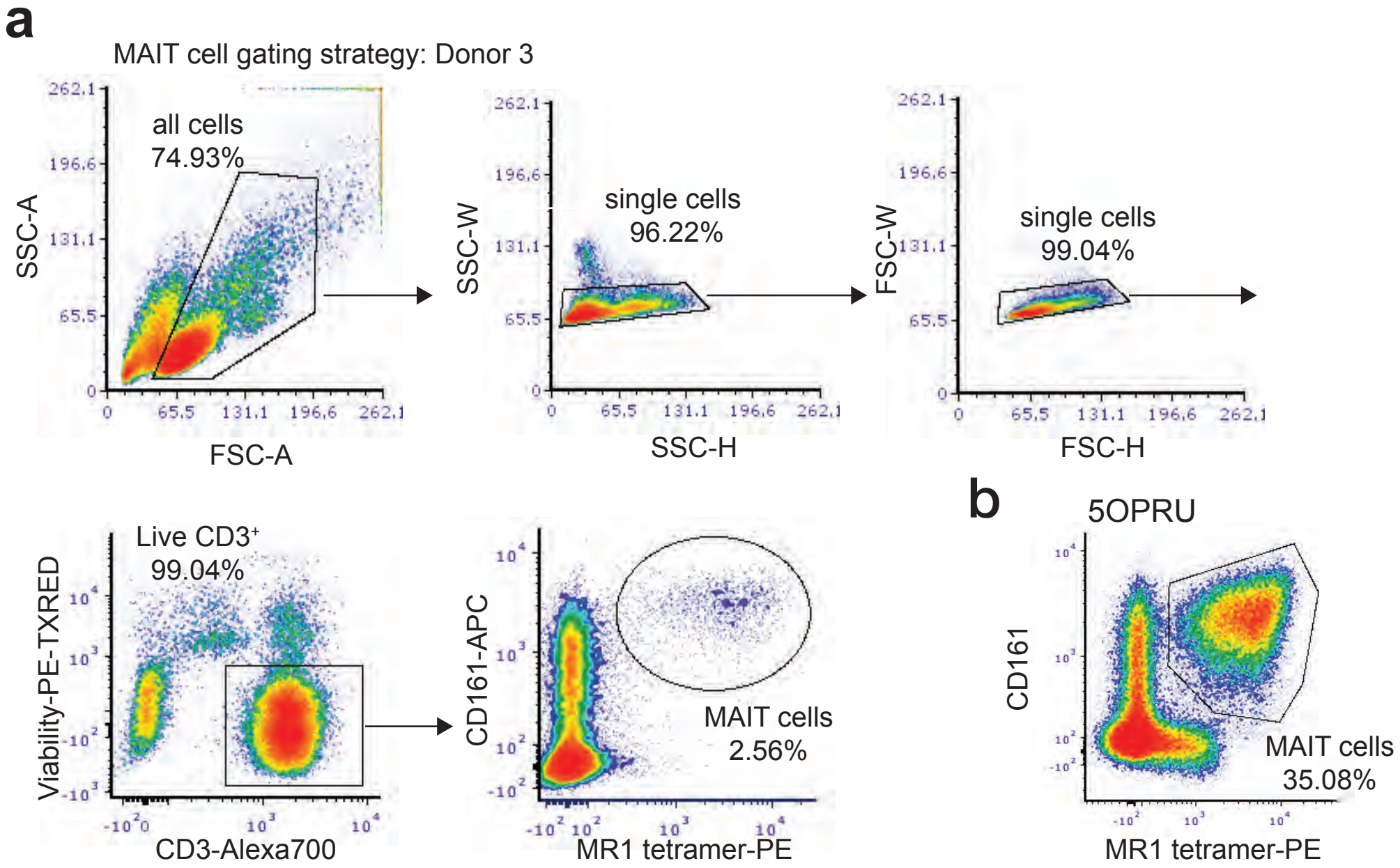

763 **Supplementary Figure 1. Flow cytometric gating strategy for MAIT cell identification.**

764

765 **(a)** Flow cytometric gating strategy to identify MAIT cells as live, $CD3^{+}$, MR1-5OPRU $tetramer^{+}$,

766 $CD161^{++}$ cells after 15 hrs of overnight rest from thaw in one donor. **(b)** MAIT cell expansion

767 within the $CD3^{+}$ T cell subset after 7 days of 5OPRU incubation.

768

Supplementary Table 1

a

MAIT cells sorted per condition

Condition	Cytokine	Donor 1	Donor 2	Donor 3
D1_REST	IL2	11,351	26,751	37,295
D1_5OPRU	IL2	11,500	25,023	13,160
D1_αCD23/CD28	IL2	7,050	15,163	33,642
D7_REST	IL2	7,236	21,201	100,000
D7_5OPRU	IL2	53,097	100,000	100,000
D7_αCD23/CD28	IL2	4,087	20,967	100,000
D7_REST	IL2/TGFβ	12,020	19,292	100,000
D7_5OPRU	IL2/TGFβ	30,900	100,000	100,000
D7_αCD23/CD28	IL2/TGFβ	4,056	15,268	75,172

b

%MAIT cells of T cells per condition

Condition	Cytokine	Donor 1	Donor 2	Donor 3
D1_REST	IL2	0.4	0.4	2.8
D1_5OPRU	IL2	0.2	0.3	0.3
D1_αCD23/CD28	IL2	0.4	0.3	1.1
D7_REST	IL2	1.0	0.5	2.6
D7_5OPRU	IL2	5.1	19.2	22.5
D7_αCD23/CD28	IL2	0.4	0.5	3.8
D7_REST	IL2/TGFβ	1.2	0.6	2.9
D7_5OPRU	IL2/TGFβ	2.7	9.1	10.9
D7_αCD23/CD28	IL2/TGFβ	0.3	0.5	2.9

774 **Supplementary Table 1. Table of MAIT cell absolute numbers and % of $CD3^+$ T cells sorted.**

775 Sorted MAIT cells per condition expressed as **(a)** absolute number and **(b)** % of total $CD3^+$ T

776 cells.

777

Supplemental Figure 2

a

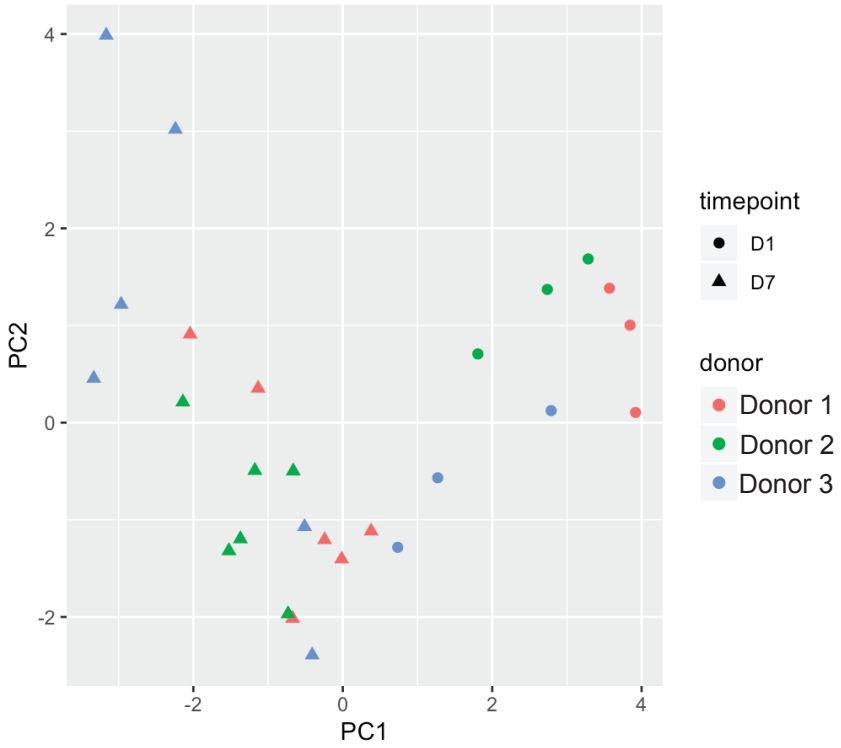

b

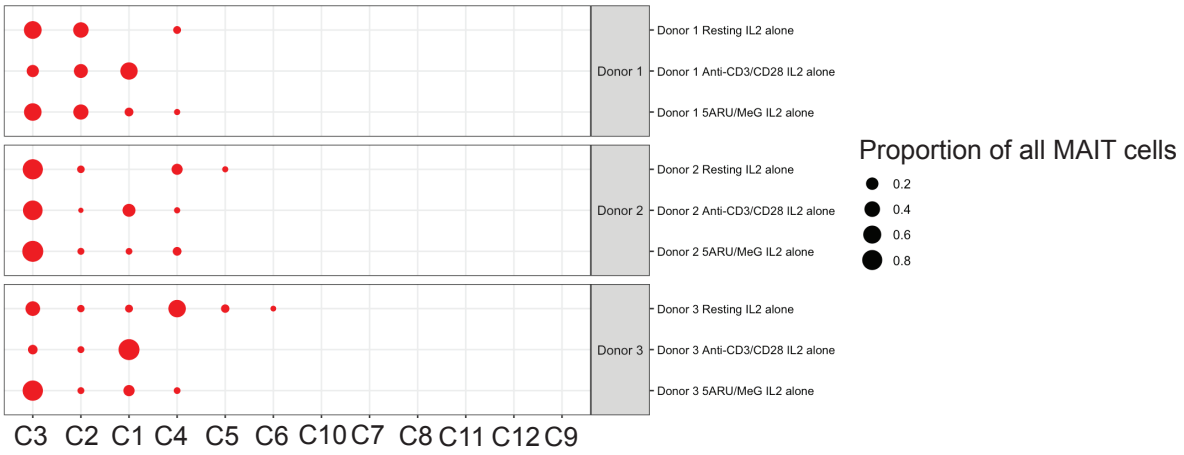

c

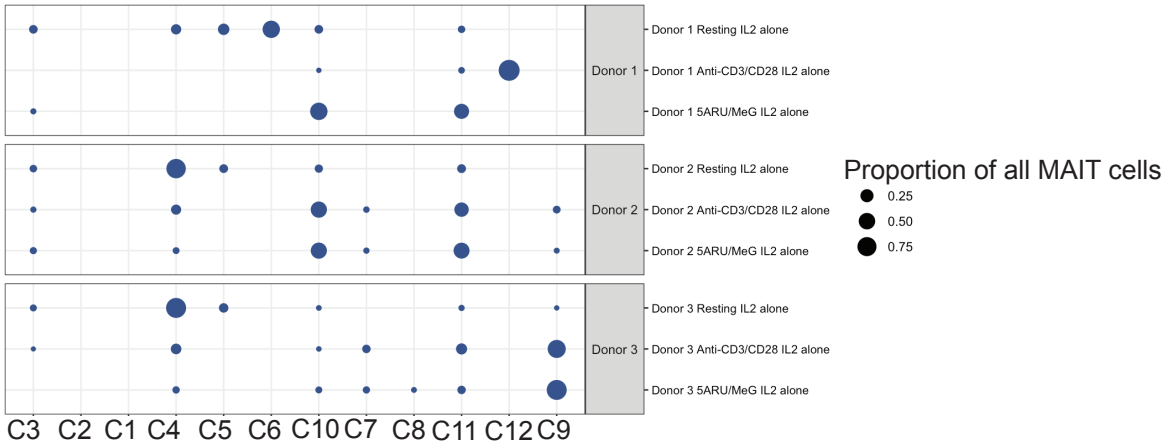

769 **Supplementary Figure 2. Single cell cluster prevalence per donor and timepoint**

770

771 **(a)** PCA of CLR-transformed cluster prevalence. Data show broad clustering by timepoint. **(b)**

772 Cluster prevalence per donor and stimulation.

773

778 **Supplementary Table 2. Differential expression gene analysis of $CD4^+$ versus $CD8^+$ MAIT**

779 **cells in the resting condition at D1 and D7, with all donors pooled together and for**

780 **individual donors**

781

782 **Supplementary Table 3. Differentially expressed genes for each cluster presented in**

783 **Figure 2.**

784

785 **Supplementary Table 4. Differential expression gene analysis of MAIT cells stimulated with**

786 **5OPRU or aCD3/CD28 at D1 and D7, with all donors pooled together and for individual**

787 **donors.**

788

789

790